*Electronic Supplementary Information*

# Thiadiazole-functionalized metal–organic frameworks for photocatalytic C−N and C−C coupling reactions: Tuning ROS generation efficiency via cobalt introduction

Kun Wu,[a] Ji-Kang Jin,[a] Xin-Yi Liu,[a] Yong-Liang Huang,[b] Pei-Wen Cheng,[a] Mo Xie,[a] Ji Zheng,[a] Weigang Lu,*[a] and Dan Li*[a]

[a] College of Chemistry and Materials Science, Guangdong Provincial Key Laboratory of Functional Supramolecular Coordination Materials and Applications, Jinan University, Guangzhou, Guangdong 510632, P. R. China

[b] Department of Chemistry, Shantou University Medical College, Shantou, Guangdong 515041, P.R. China

E-mail: weiganglu@jnu.edu.cn, danli@jnu.edu.cn

## Contents

## Section 1. General

### 1.1. Materials and physical measurements

All reagents and solvents were purchased from commercial sources and used as received. $Co(NO_3)_2 \cdot 6H_2O$, solvents and organic substrates were purchased from Energy Chemical, Shanghai tengzhun Biotechnology Co., Ltd and Sigma-Aldrich Co., Inc. All heating reactions were heated by metal sand bath (WATTCAS, LAB-500, https://www.wattcas.com). The ligand 4,7-di(1H-pyrazol-4-yl)benzo[*c*][1,2,5]thiadiazole ($H_2$PBT) was synthesized using our previously reported procedure. Fourier transform infrared (FT−IR) spectra were collected on a Thermo Scientific Nicolet iS10 spectrophotometer in the range of 4000−400 $cm^{-1}$. Powder X-ray diffraction (PXRD) was performed on Rigaku Ultima IV diffractometer (Cu K$\alpha$ radiation, $\lambda$ = 1.5406 Å). Single-crystal X-ray diffraction (SCXRD) data were collected at 100 K, via an Oxford Cryo stream system on a XtaLAB PRO MM007-DW diffractometer system equipped with a RA-Micro7HF-MR-DW(Cu/Mo) X-ray generator and HyPix-6000HE Hybrid Photon Counting (HPC) X-ray detector (Rigaku, Japan, Cu Kα, graphite monochromator, $\lambda$ = 1.54 Å). CCDC-2173247 contain the supplementary crystallographic data for this paper. These data can be obtained free of charge from the Cambridge Crystallographic Data Centre www.ccdc.cam.ac.uk/structures. Thermogravimetric analysis (TGA) curves were obtained on Mettler-Toledo (TGA/DSC) thermal analyzer from 40 °C to 800 °C with a heating rate of 10 °C $min^{-1}$ under a nitrogen gas atmosphere (20 mL·$min^{-1}$). Nitrogen gas adsorption/desorption measurements were performed on Micromeritics ASAP 2020 Plus adsorption instrument UV−Visible diffuse reflection spectra were recorded on Agilent Cary 4000 with $BaSO_4$ as the reference. X-ray photoelectron spectroscopy (XPS) data were collected on a Thermo ESCALAB 250XI system. Solid- and solution-state luminescence spectra were measured on Horiba FluoroLog-3 spectrofluorometer. Decay curve was measured on Horiba FluoroMax-4 fluorometer with a NanoLED-455 flash lamp.

### 1.2. Synthesis of ligand $H_2PBT$

1,4-bis(1H-pyrazol-4-yl) benzothiadiazole ($H_2PBT$) was synthesized according to our previously reported method.[1]

To a solution of 4,7-dibromobenzo[*c*][1,2,5]thiadiazole (1.0 g, 3.4 mmol) $K_2CO_3$ (4.37 g, 31.64 mmol) and $Pd(PPh_3)_4$ (110.4 mg, 0.078 mmol) in 80 mL of 1,2-Dimethoxyethane (DME). After being stirred and refluxed for 24 h at 80 °C under Ar. After the reaction is complete, the solvent was removed in vacuo. The obtained orange solid was separated and purified by column chromatography (EtOAc : PE = 1: 3) to obtain a large amount of orange yellow solid, which was the intermediate 4,7-bis(1-(tetrahydro-2H-pyran-2-yl)-1H-pyrazol-4-yl)benzo[*c*][1,2,5]thiadiazole with yield of about 88%.

$^1$H NMR (400MHz, $CDCl_3$): δ = 1.75 (m, 6H), 2.19 (m, 6H), 3.78 (m, 2H), 4.15 (dd, 2H), 5.51 (dd, 2H), 7.79 (s, 2H), 8.26 (s, 2H), 8.73 (s, 2H) ppm. $^{13}$C NMR (100 MHz, $CDCl_3$): δ = 22.45, 24.98, 30.58, 67.92, 87.92, 119.04, 123.39, 124.59, 127.87, 137.8, 153.14 ppm.

To a solution of intermediate (1.22 g, 4.25mmol) in EtOH (50 mL), add HCl (25 mL, 1M), the resulting mixture was refluxed for 10 h at 80 °C. After the reaction is complete, the precipitate was filtered and washed with EtOH. Pour the obtained solid into a beaker containing 100 mL of distilled water, adjust the pH to 5−7 with NaOH (0.5 M), filter, and wash with distilled water to neutral. Then rinse with a small amount of ethanol and ether to afford $H_2PBT$ as a dark-yellow solid $H_2PBT$ with yield of about 95%. $^1$H NMR (400 MHz, $d_6$-DMSO): δ = 8.53 (s, 4H), 8.01 (s, 2H). $^{13}$C NMR (100 MHz, $d_6$-DMSO): δ = 153.53, 133.21, 125.31, 123.50, 117.76 ppm. IR (KBr, $cm^{-1}$): 3133(m), 3045(m), 2950(w), 2741(w), 1685(w), 1590(s), 1576(w), 1560(w), 1519(s), 1396(w), 1357(m), 1335(m), 1276(m), 1243(m), 1152(m), 1045(m), 1005(s), 958(s), 884(s), 853(m), 835(s), 672(w), 605(s), 553(m), 540 (w), 505(w).

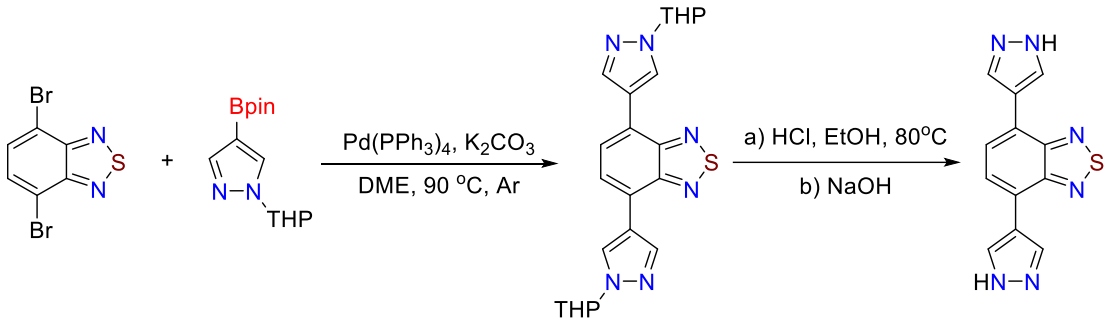


Fig. S1. The synthesis procedure of ligand $H_2$PBT.

### 1.3. Synthesis of JNU-207

A mixture of $H_2$PBT (4,7-di(1H-pyrazol-4-yl)benzo[*c*][1,2,5]thiadiazole, 6 mg, 0.02 mmol), $Co(NO_3)_3 \cdot 6H_2O$ (5.8 mg, 0.02 mmol), *N, N*-dimethylformamide (DMF, 3 mL), and $HNO_3/H_2O$ (12/50 mL, 130 $\mu$L) was sealed in a 10 mL glass vial and placed in an oven at 120 °C for 72 h. After cooling to room temperature, the black prismatic crystals of **JNU-207** were collected (46% yield, based on $H_2$PBT). The fresh crystalline samples were solvent exchanged with DMF and EtOH for three days and then heated up to 100 °C overnight before the next use. FT-IR ($cm^{-1}$): $\nu$ = 3351.34 (w), 1664 (s), 1587 (s), 1546 (s), 1406 (w), 1376 (m), 1295 (w), 1248 (s), 1172 (w), 1052 (s), 1016 (m), 880 (m), 834 (s), 643 (w), 610 (s), 544 (s), 470 (m), 463 (m).

Note that **JNU-207** can also be obtained using a thick-walled pressure flask heated in a sand bath and this method can be scaled up appropriately. $H_2$PBT (0.11 mmol, 29.5 mg) and $Co(OAc)_2 \cdot 4H_2O$ (0.19 mmol, 48 mg) were dissolved in 8.0 mL DMF and 4.0 mL water in a 25 mL thick-walled pressure flask. The flask was then tightly sealed and the resulting suspension was heated in a sand bath at 150 °C for 12 h. After cooling naturally to room temperature, and the target product was obtained.

Fig. S2. All heating reactions were heated by metal sand bath (WATTCAS, LAB-500).

## Section 2. Characterization of JNU-207

### 2.1 Crystallographic data

Single crystal structures of MOFs were measured by X-ray diffraction at 100 K on XtaLAB PRO MM007-DW diffractometer system equipped with a RA-Micro7HF-MR-DW(Cu/Mo) X-ray generator and HyPix-6000HE Hybrid Photon Counting (HPC) X-ray detector (Rigaku, Japan, Cu K$\alpha$, graphite monochromator, $\lambda$ = 1.54178 Å). The structure was solved by direct methods and refined by full-matrix least-squares refinements based on $F^2$. Anisotropic thermal parameters were applied to all non-hydrogen atoms. The crystallographic calculations were performed using Olex 2 with 'XL' plugins. CCDC-2173247 (**JNU-207**), contain the supplementary crystallographic data for this paper.

**Table S1**. Crystal data and structure refinement for **JNU-207**.

| MOF | **JNU-207** |
|---|---|
| CCDC number | 2173247 |
| Empirical formula | $C_{12}H_6N_6SCo$ |
| Formula weight | 319.29 |
| Crystal system | tetragonal |
| Space group | $I4_122$ |
| *a*/Å | 16.5978(2) |
| *b*/Å | 16.5978(2) |
| *c*/Å | 12.3112(2) |
| V/Å$^3$ | 3391.58(10) |
| $\alpha$/° | 90 |
| $\beta$/° | 90 |
| $\gamma$/° | 90 |
| Z | 8 |
| $D_C$/g cm$^{-3}$ | 1.274 |
| $\mu$/mm$^{-1}$ | 9.079 |
| $\lambda$/Å | 1.54184 |
| T/K | 100 |
| Reflections collected | 6012 |
| Independent reflections | 1758 [$R_{int}$ = 0.0331] |
| Goodness-of-fit on $F^2$ | 1.089 |
| $R_1$[a], $wR_2$[b] [ I > 2$\sigma$ (I)] | $R_1$ = 0.0795, $wR_2$ = 0.2213 |
| $R_1$[a], $wR_2$[b] (all data) | $R_1$ = 0.0823, $wR_2$ = 0.2240 |
| Largest diff. peak and hole /e. Å$^{-3}$ | 0.62/−0.83 |
| Flack parameter | 0.037(14) |

[a] $R_1 = \Sigma||F_o|-|F_c|| / \Sigma|F_o|$

[b] $wR_2 = \{\Sigma[w (F_o^2-F_c^2)^2]/[w (F_o^2)^2]\}$ 1/2, [$F_o > 4\sigma (F_o)$]

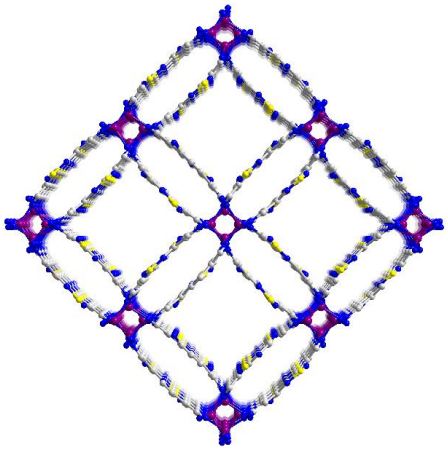

Fig. S3. Views of **JNU-207** along the [001] direction with uniformed square 1D channels (colour code: C, gray; N, blue; S, yellow and Co, violet; H atoms are omitted for clarity).

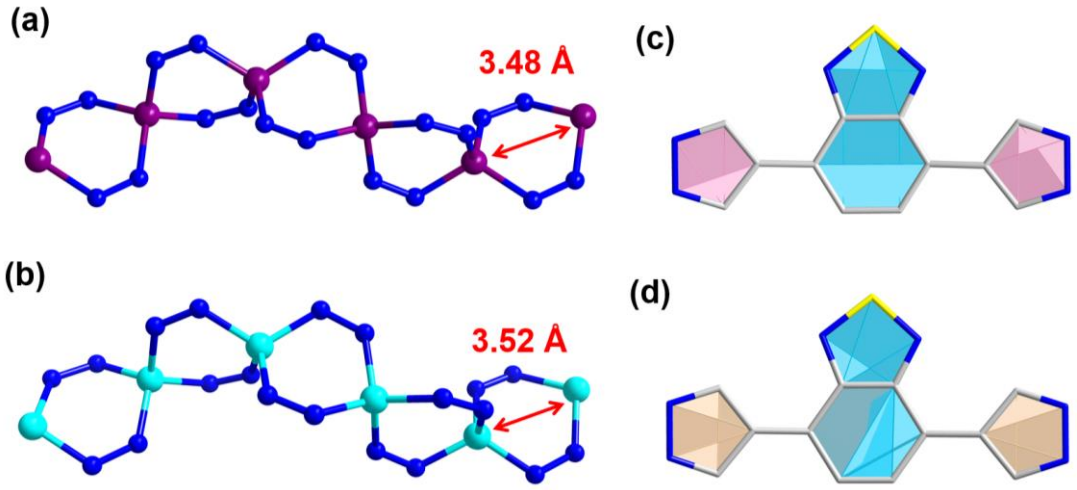


Fig. S4. (a) $CoN_4$ and (b) $ZnN_4$ clusters are connected through edge-sharing pyrazoles to form helical rod SBUs. Linker distortion between the pyrazole plane and the benzothiadiazole plane (c) **JNU-207** and (d) **JNU-204** (Co, violet; Zn, sky blue; C, gray; N, blue; H atoms are omitted for clarity).

## 2.2. Additional characterization

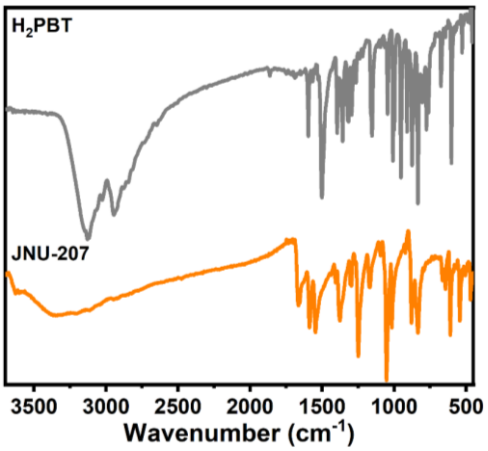


Fig. S5. FT-IR spectra of $H_2$PBT and **JNU-207**.

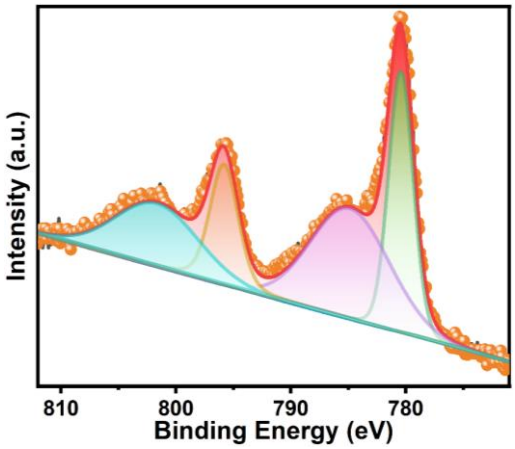


Fig. S6. High resolution XPS spectra of Co elements in **JNU-207**.

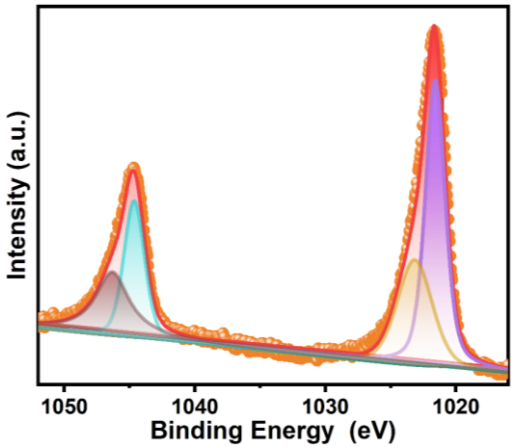


Fig. S7. High resolution XPS spectra of Zn elements in **JNU-204**.

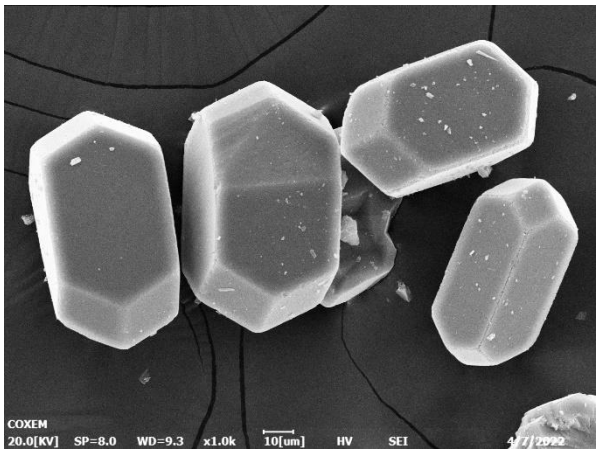


Fig. S8. SEM image of **JNU-207**.

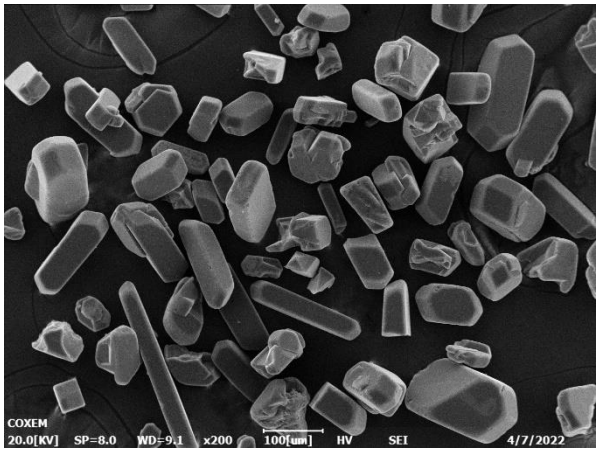


Fig. S9. SEM image of **JNU-204**.

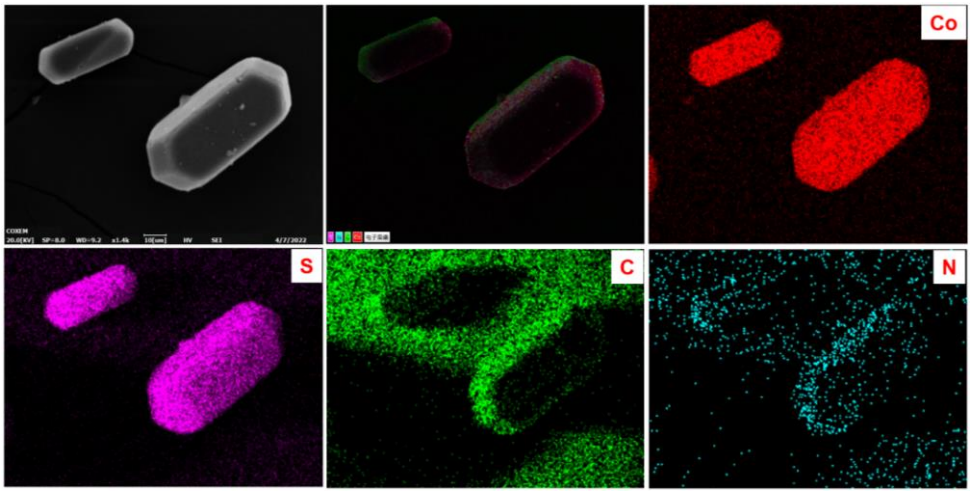


Fig. S10. SEM-EDS mapping and EDS spectra profiles of **JNU-207**.

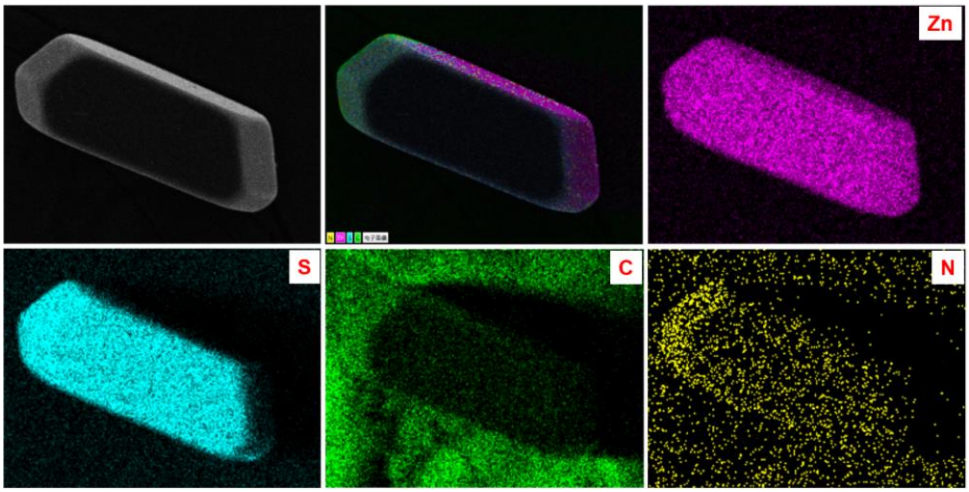


Fig. S11. SEM-EDS mapping and EDS spectra profiles of **JNU-204**.

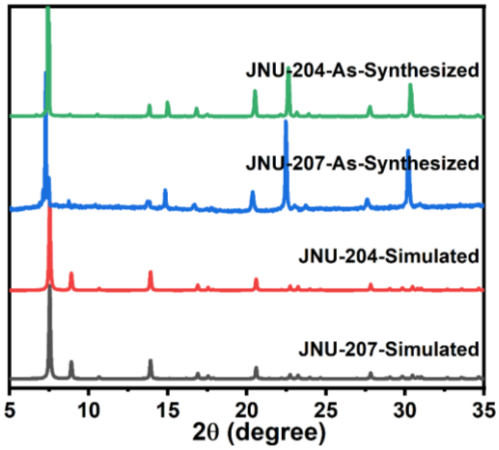


Fig. S12. Comparison of the PXRD patterns of **JNU-207** and **JNU-204**.

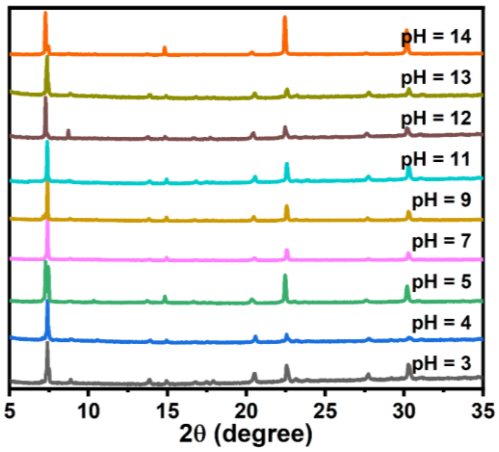


Fig. S13. Comparison of the PXRD patterns of **JNU-207** after being treated with different aqueous solutions at different pH values.

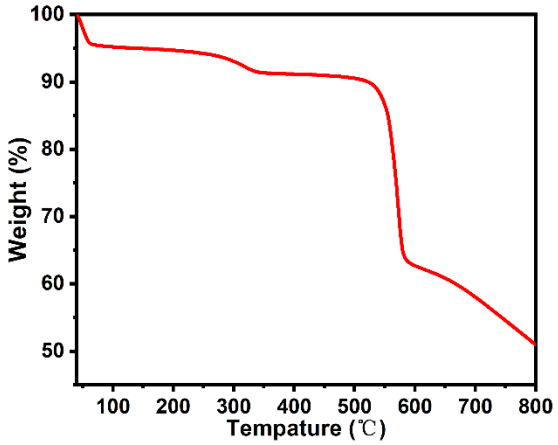


Fig. S14. Thermogravimetric analysis (TGA) of **JNU-207**.

### 2.3. Electrochemical measurements.

10 mg of the MOF was ground and added into 100 $\mu$L of ethanol and 10 $\mu$L of Nafion (5 wt%), sonicated for 30 min to afford a finely dispersed suspension. Then, the obtained suspension was coated on the surface of fluorine-doped tin oxide (FTO) glass, scraped into a uniform film and dried for 0.5 hours. The electrochemical measurements were performed in a conventional three-electrode cell on a CHI-760E electrochemical workstation (Shanghai Chenhua Instrument Co., Ltd, China), with the MOF-coated FTO glass as working electrode, Pt wire as the counter electrode, and Ag/AgCl as the reference electrode. 300W Xe lamp (China Education Au-light, CEL−HXF300/CEL−HXUV300) coupled with a UV cutoff filter ($\lambda \geq 420$ nm) was used to simulate the visible light for the photocurrent measurements. The photo-responsive signals were measured under visible light irradiation at 0.4 V in a 0.5 M $Na_2SO_4$ solution, and Mott Schottky plots were made by using three different frequencies, 1000, 2000, and 3000 Hz. Electrochemical impedance spectroscopy (EIS) measurements were carried out in a 0.5 M $Na_2SO_4$ solution, the amplitude of the sinusoidal wave was 5 mV with frequency ranging from 100 kHz to 0.05 Hz.

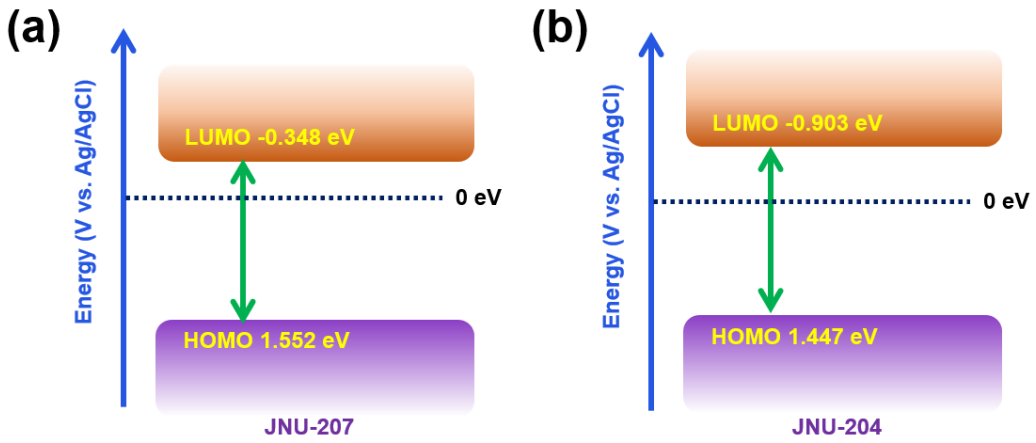


Fig. S15. Schematic depiction of the optical band gap of **JNU-207** and **JNU-204**.

Table S2. Fitting data of the photoluminescence decay of **JNU-207** and **JNU-204**.

| | A1 | A2 | A3 | $\tau_1$ | $\tau_2$ | $\tau_3$ | $\tau_{av}$ | Chi2 |
|---|---|---|---|---|---|---|---|---|
| **JNU-207** | 0.6253725 | 2.551819E-02 | 5.612912E-05 | 1.827734E-10 sec | 1.840305E-09 sec | 6.459449E-08 sec | 0.25 ns | 1.54 |
| **JNU-204** | 0.2242236 | 5.310204E-02 | 1.372023E-04 | 1.152505E-09 sec | 2.495059E-09 sec | 9.16784E-08 sec | 1.45 ns | 1.33 |

$\tau_{av} = (A1 \times \tau_1^2 + A2 \times \tau_2^2 + A3 \times \tau_3^2)/(A1 \times \tau_1 + A2 \times \tau_2 + A3 \times \tau_3)$.

## Section 3. Photocatalytic Application

### 3.1 photocatalytic synthesis of imines

General procedure A:

A solution of primary amine (**1**) (1.001 mmol) and **JNU-207** (1 mol%) in $CH_3CN$ (5 mL) was stirred under blue LED for 24 h at room temperature. After evaporation of solvent, the crude residue was dissolved in $CDCl_3$ along with 20 $\mu$L $CHCl_2CHCl_2$ as internal standard for crude NMR.

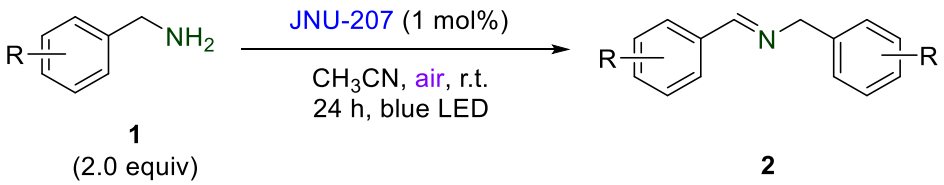


A solution of benzylamine (**1a**) (126.4 μL, 1.001 mmol), **JNU-207** (1 mol%) in $CH_3CN$ (5 mL) was stirred under blue LED for 24 h at room temperature. After

evaporation of solvent, the crude residue was dissolved in $CDCl_3$ along with 20 $\mu$L $CHCl_2CHCl_2$ as internal standard for crude NMR. Based on crude $^1H$ NMR, the desired product **2a** was detected in 94% yield.

**(*E*)-*N*-benzyl-1-phenylmethanimine (2a)**

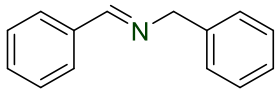


NMR yield: 94%. $^1H$ NMR (400 MHz, $CDCl_3$) 4.81 (2H, s), 7.26-7.33 (8H, m), 7.68-7.87 (2H, m), 8.38 (1H, s).

**(*E*)-*N*-(4-methylbenzyl)-1-(*p*-tolyl)methanimine (2b)**

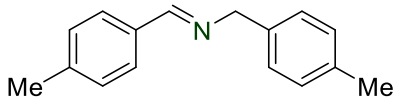


NMR yield: 80%. $^1H$ NMR (400 MHz, $CDCl_3$) 2.24 (3H, s), 2.28 (3H, s), 4.67 (2H, s), 7.04-7.14 (6H, m), 7.57 (2H, d, $J$ = 8.0 Hz), 8.24 (1H, s).

**(*E*)-*N*-(4-butylbenzyl)-1-(4-butylphenyl)methanimine (2c)**

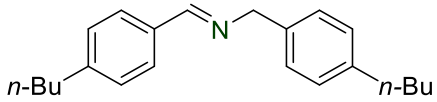


NMR yield: 95%. $^1H$ NMR (400 MHz, $CDCl_3$) 0.97-1.01 (6H, m), 1.37-1.46 (4H, m), 1.61-1.71 (4H, m), 2.64-2.71 (4H, m), 4.83 (2H, s), 7.21 (2H, d, $J$ = 8.0 Hz), 7.26-7.31 (4H, m), 7.75 (2H, d, $J$ = 8.4 Hz), 8.40 (1H, s).

**(*E*)-*N*-(4-methoxybenzyl)-1-(4-methoxyphenyl)methanimine (2d)**

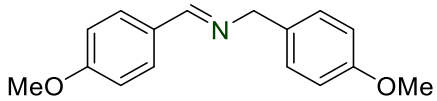

NMR yield: 88%. $^1$H NMR (400 MHz, $CDCl_3$) 3.70 (3H, s), 3.74 (3H, s), 4.64 (2H, s), 6.79 (2H, d, $J$ = 8.4 Hz), 6.84 (2H, d, $J$ = 8.8 Hz), 7.26 (2H, d, $J$ =8.8 Hz), 7.63 (2H, d, $J$ = 8.8 Hz), 8.21 (1H, s).

**(*E*)-*N*-(4-chlorobenzyl)-1-(4-chlorophenyl)methanimine (2e)**

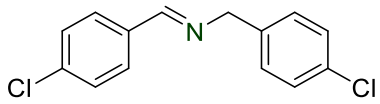


NMR yield: 88%. $^1$H NMR (400 MHz, $CDCl_3$) 4.75 (2H, s), 7.21-7.31 (6H, m), 7.37 (2H, d, $J$ = 8.8 Hz), 7.69 (2H, d, $J$ = 8.4 Hz), 8.32 (1H, s).

**(*E*)-*N*-(4-fluorobenzyl)-1-(4-fluorophenyl)methanimine (2f)**

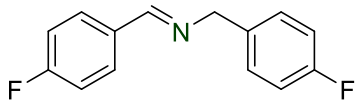


NMR yield: 96%. $^1$H NMR (400 MHz, $CDCl_3$) 4.67 (2H, s), 6.94 (2H, dddd, $J$ = 2.0, 2.8, 8.4, 8.8 Hz), 7.01 (2H, dddd, $J$ = 2.0, 2.8, 8.4, 8.8 Hz), 7.20 (2H, dddd, $J$ = 2.0, 2.8, 5.2, 8.4 Hz), 7.68 (2H, dddd, $J$ = 2.0, 2.8, 5.2, 8.4 Hz), 8.25 (1H, s).

**(*E*)-*N*-(3-methylbenzyl)-1-(*m*-tolyl)methanimine (2g)**

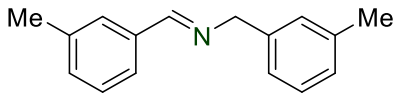


NMR yield: 89%. $^1$H NMR (400 MHz, $CDCl_3$) 2.33 (3H, s), 2.36 (3H, s), 4.76 (2H, s), 7.05-7.13 (3H, m), 7.19-7.23 (2H, m), 7.29 (1H, dd, $J$ = 7.2, 7.6 Hz), 7.53 (1H, d, $J$ = 7.6 Hz), 7.63 (1H, s), 8.33 (1H, s).

**(*E*)-*N*-(2-methylbenzyl)-1-(*o*-tolyl)methanimine (2h)**

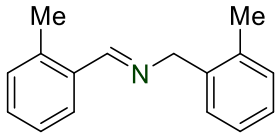


NMR yield: 81%. $^1$H NMR (400 MHz, $CDCl_3$) 2.38 (3H, s), 2.49 (3H, s), 4.81 (2H, s), 7.15-7.28 (7H, m), 7.92 (1H, d, $J$ = 7.6), 8.65 (1H, s).

**Table S3**. Representative heterogeneous porous catalysts for the oxidative coupling of benzylamines.

| Catalyst | Reaction conditions | Yield | Reference |
|---|---|---|---|
| MOF-6 ($Ru(bpy)_3^{2+}$ | 38$\mu$l [B], 1 mol % [P], 3 mL $CH_3CN$, 300W Xe lamp $O_2$, 60 ℃ 1h | 83% | 2 |
| $NH_2$-MIL125(Ti) | 0.1 mmol [B], 5 mg [P], 2 mL $CH_3CN$, 300W Xe lamp, $O_2$, 12h | 73% | 3 |
| PCN-222 (Zr) | 0.1 mmol [B], 5 mg [P], 3 mL $CH_3CN$, 300W Xe lamp, air, 1h | 100% | 4 |
| UNLPF-12 (Zr) (SnIVporphyrin) | 0.27 mmol [B], 1.0 μmol [P], 1 mL dry $CH_3CN$, 14 W CFL, air, 2h | 99% | 5 |
| Zn-PDI | 1 mmol [B], 1 mol% [P], 5 mL $CH_3CN$, 500W Xe lamp air, 4h | 74% | 6 |
| [In(OH)(ADBEB)]·DMF | 0.2 mmol [B], 4 mg [P], 1 mL DMSO, visible light, $O_2$, 2.67 h | 99% | 7 |
| Cd-MOF | 0.48 mmol [B], 10 mg [P], 5 mL DMF, 300 W Xe lamp air, 7 h | 99.1% | 8 |
| ZIF-8 | 11 $\mu$L [B], 10 mg [P], 1 mL anhydrous DMF, 450 nm LED, $O_2$, 7h | 3.5% | 9 |
| UiO-66 | 11 $\mu$L [B], 10 mg [P], 1 mL dry DMF, 450 nm LED, $O_2$, 7h | 3.0% | 9 |
| MIL-125 | 11 $\mu$L [B], 10 mg [P], 1 mL dry DMF, 450 nm LED, $O_2$, 7h | 3.3% | 9 |
| NP5-DM-COF | 0.2 mmol [B], 3 mg [P], 2 mL $CH_3CN$, 30W LED, r.t., | 99% | 10 |

| | | | |
|---|---|---|---|
| | $O_2$, 15h | | |
| $Zn_2(DPNDI)(W_{10}O_{32})(DMA)_6$ | 0.4 mmol [B], 1 mol% [P], 2 mL DMF,100 W white LED lamp, $O_2$, 24h | 99% | 11 |
| RPF-30-Er | 0.05 mmol [B], 10 mol% [P], 1 mL $CH_3CN$, 100 W warming lamp $O_2$, 18h | 76% | 12 |
| ZJU-56-0.2 | 1 mmol [B], 1.0 mol % [P], 2 mL $CH_3CN$, 660 nm LEDs, 60 ℃, $O_2$, 24h | 62% | 13 |
| Ni MOF-74 nanosheets | 0.1 mmol [B], 10 mg [P], 2 mL $CH_3CN$, 300 W Xenon Lamp, $O_2$, 4 h | 91.6% | 14 |
| FJI-Y10 | 1 mmol [B], 2 mmol % [P] basing on the L, 5 mL DMF, 300 W Xe lamp, 40 °C, $O_2$, 6 h. | 100% | 15 |
| $Zn_2(diPyPI\text{-}Cl_4)(NDC)_2\cdot 3DMF$ | 0.2 mmol [B], 0.5 mol% [P], 300W Xe lamp $O_2$, r.t., 6h | 100% | 16 |
| JNU-204 | 1 mmol [B], 1mol% [P], 5mL $CH_3CN$, blue LED, air, r.t., 24h | 86% | This work |
| JNU-207 | 1 mmol [B], 1mol% [P], 5mL $CH_3CN$, blue LED, air, r.t., 24h | 94% | This work |

[B] = benzylamine; [P] = photocatalyst; r.t. = room tempature.

### 3.2 photocatalytic synthesis of tetrahydroquinolines

General procedure B:

A solution of tertiary amine (**3**) (1.001 mmol), maleimide (**4**) (0.501 mmol), **JNU-207** (1 mol%) in DMF (5 mL) was stirred under blue LED for 48 h at room temperature. After completion of the reaction, the reaction was extracted with ethyl acetate. The combined organic layer was washed with brine, dried over $Na_2SO_4$, filtered and concentrated. The crude residue was dissolved in $CDCl_3$ along with 20 $\mu$L $CHCl_2CHCl_2$ as internal standard for crude NMR.

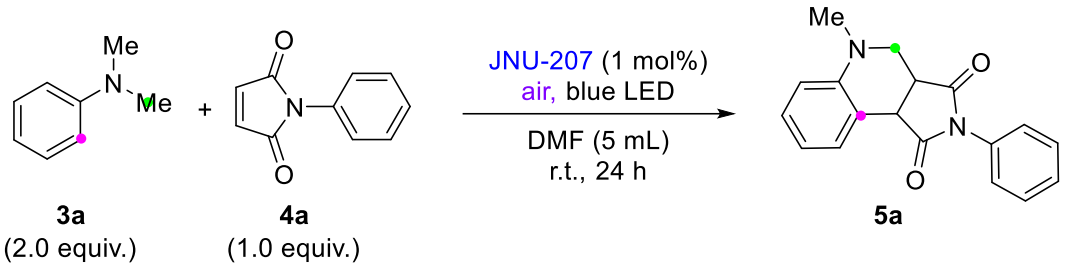


**3a** (2.0 equiv.) **4a** (1.0 equiv.) **5a**

A solution of *N*,*N*-Dimethylaniline (3a) (126.4 μL, 1.001 mmol), *N*-Phenylmaleimide (4a) (86.7 mg, 0.501 mmol), **JNU-207** (1 mol%)) in DMF (5 mL) was stirred under blue LED for 48 h at room temperature. After completion of the reaction, the reaction was extracted with ethyl acetate. The combined organic layer was washed with brine, dried over $Na_2SO_4$, filtered and concentrated. The crude residue was dissolved in $CDCl_3$ along with 20 μL $CHCl_2CHCl_2$ as internal standard for crude NMR. Based on crude $^1$H NMR, the desired cyclization product **5a** was detected in 78% yield.

**5-Methyl-2-phenyl-3a,4,5,9b-tetrahydro-1*H*-pyrrolo[3,4-*c*]quinoline-1,3(2*H*)-dione (5a)**

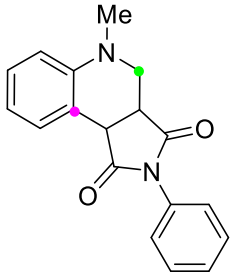


NMR Yield: 77%. $^1$H NMR (400 MHz, $CDCl_3$) δ 2.75 (3H, s), 3.03 (1H, dd, *J* = 4.4, 11.6 Hz), 3.42-3.46 (1H, m), 3.52 (1H, dd, *J* = 2.4, 11.2 Hz), 4.06 (1H, d, *J* = 9.6 Hz), 6.67 (1H, d, *J* = 8.0 Hz), 6.83 (1H, dd, *J* = 7.2, 7.6 Hz), 7.13-7.18 (3H, m), 7.27 (1H, dd, *J* = 7.2, 7.2 Hz), 7.34 (2H, dd, *J* = 7.2, 8.0 Hz), 7.44 (1H, d, *J* = 7.2 Hz); $^{13}$C NMR (100 MHz, $CDCl_3$) δ = 39.4, 42.0, 43.4, 50.6, 112.6, 118.5, 119.7, 126.3, 128.5, 128.6, 128.9, 130.3, 131.9, 148.4, 175.7, 177.6.

**2-(4-Methoxyphenyl)-5-methyl-3a,4,5,9b-tetrahydro-1*H*-pyrrolo[3,4-*c*]quinoline-1,3(2*H*)-dione (5b)**

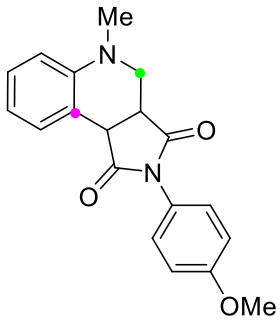


NMR Yield: 76%. $^{1}$H NMR (400 MHz, $CDCl_3$) δ 2.87 (3H, s), 3.16 (1H, dd, *J* = 4.4, 11.6 Hz), 3.53-3.58 (1H, m), 3.63 (1H, dd, *J* = 2.8, 11.2 Hz), 3.83 (3H, s), 4.17 (1H, d, *J* = 9.6 Hz), 6.78 (1H, d, *J* = 8.0 Hz), 6.92-6.97 (3H, m), 7.20 (2H, ddd, *J* = 3.0, 3.2, 9.2 Hz), 7.26 (1H, dd, *J* = 7.2, 8.4 Hz), 7.56 (1H, d, *J* = 7.2 Hz); $^{13}$C NMR (100 MHz, $CDCl_3$) δ = 39.5, 42.0, 43.4, 50.6, 55.5, 112.7, 114.3, 118.7, 119.8, 124.6, 127.6, 128.7, 130.3, 148.3, 159.4, 175.9, 177.9.

**2-(4-Chlorophenyl)-5-methyl-3a,4,5,9b-tetrahydro-1*H*-pyrrolo[3,4-*c*]quinoline-1, 3(2*H*)-dione (5c)**

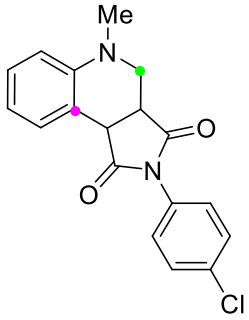


NMR Yield: 77%. $^{1}$H NMR (400 MHz, $CDCl_3$) δ 2.77 (3H, s), 3.05 (1H, dd, *J* = 4.4, 11.2 Hz), 3.45-3.49 (1H, m), 3.54 (1H, dd, *J* = 2.8, 11.6 Hz), 4.09 (1H, d, *J* = 9.6 Hz), 6.68 (1H, d, *J* = 8.0 Hz), 6.84 (1H, ddd, *J* = 0.8, 7.2, 7.6 Hz), 7.15-7.19 (3H, m), 7.32 (2H, ddd, *J* = 2.0, 2.8, 8.8 Hz), 7.45 (2H, d, *J* = 7.2 Hz); $^{13}$C NMR (100 MHz, $CDCl_3$) δ = 39.5, 42.0, 43.4, 50.6, 55.5, 112.7, 114.3, 118.7, 119.8, 124.6, 127.6, 128.7, 130.3, 148.3, 159.4, 175.9, 177.9.

**5-Methyl-2-(*m*-tolyl)-3a,4,5,9b-tetrahydro-1*H*-pyrrolo[3,4-*c*]quinoline-1,3(2*H*)-dione (5d)**

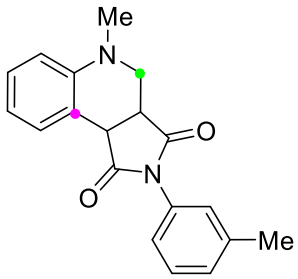


NMR Yield: 72%. $^{1}$H NMR (400 MHz, $CDCl_3$) δ 2.27 (3H, s), 2.77 (3H, s), 3.06 (1H, dd, *J* = 4.4, 11.6 Hz), 3.44-3.48 (1H, m), 3.54 (1H, dd, *J* = 2.4, 11.2 Hz), 4.08 (1H, d, *J* = 9.6 Hz), 6.69 (1H, d, *J* = 8.4 Hz), 6.84 (1H, dd, *J* = 7.2, 7.6 Hz), 6.97-6.98 (2H, m), 7.09 (1H, d, *J* = 7.6 Hz), 7.17 (1H, dd, *J* = 5.6, 8.0 Hz), 7.24 (1H, dd, *J* = 7.6, 8.4 Hz), 7.46 (1H, d, *J* = 7.6 Hz); $^{13}$C NMR (100 MHz, $CDCl_3$) δ = 21.3, 39.5, 42.1, 43.4, 50.6, 112.7, 118.6, 119.8, 123.4, 126.9, 128.7, 128.8, 129.4, 130.3, 131.8, 139.1, 148.3, 175.8, 177.7.

**5-Methyl-2-(*o*-tolyl)-3a,4,5,9b-tetrahydro-1*H*-pyrrolo[3,4-*c*]quinoline-1,3(2*H*)-dione (5e)**

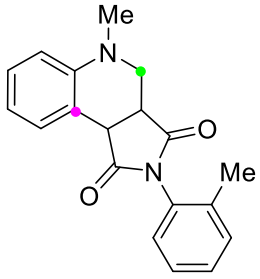


NMR Yield: 67%, a mixture of diastereomers (dr = 2:1) was obtained. $^{1}$H NMR (400 MHz, $CDCl_3$) δ 1.83 (3H, s), 2.20 (3H, s), 2.85 (3H, s), 3.09-3.16 (1H, m), 3.55-3.65 (1H, m), 4.17-4.19 (1H, m), 6.74-6.78 (1H, m), 6.89-7.14 (2H, m), 7.17-7.31 (2H, m), 7.49-7.53 (2H, m); $^{13}$C NMR (100 MHz, $CDCl_3$) δ = 17.0, 17.8, 39.2, 39.5, 42.4, 42.8, 43.7, 44.3, 50.8, 51.1, 112.3, 112.5, 118.6, 118.9, 119.7, 119.8, 126.77, 126.81, 127.8, 128.2, 128.7, 129.4, 129.5, 129.6, 130.3, 131.0, 131.1, 135.3, 135.9, 148.56, 148.60, 175.7, 175.8, 177.6, 177.9.

**2-Cyclohexyl-5-methyl-3a,4,5,9b-tetrahydro-1*H*-pyrrolo[3,4-*c*]quinoline-1,3(2*H*)-**

**dione (5f)**

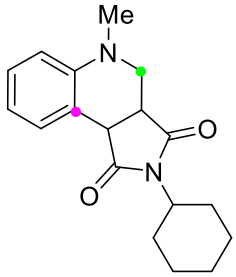


NMR Yield: 78%. $^{1}$H NMR (400 MHz, $CDCl_3$) δ 1.12-1.33 (3H, m), 1.50-1.64 (3H, m), 1.76-1.80 (2H, m), 2.01-2.17 (2H, m), 2.79 (3H, s), 3.02 (1H, dd, *J* = 4.4, 11.6 Hz), 3.25-3.29 (1H, m), 3.45 (1H, dd, *J* = 3.2, 11.6 Hz), 3.88-3.98 (2H, m), 6.69 (1H, d, *J* = 8.0 Hz), 6.88 (1H, dd, *J* = 7.2, 7.6 Hz), 7.20 (1H, ddd, *J* = 1.2, 6.8, 8.4 Hz), 7.46 (1H, d, *J* = 7.6 Hz); $^{13}$C NMR (100 MHz, $CDCl_3$) δ = 25.0, 25.69, 25.74, 28.7, 28.8, 39.3, 41.7, 43.0, 50.8, 52.1, 112.3, 119.0, 119.4, 128.3, 130.1, 148.3, 176.8, 178.6.

**5,8-Dimethyl-2-phenyl-3a,4,5,9b-tetrahydro-1*H*-pyrrolo[3,4-*c*]quinoline-1,3(2*H*)-dione (5g)**

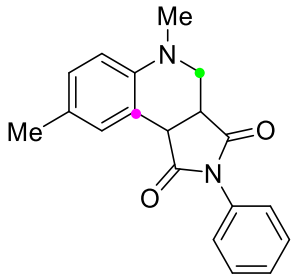


NMR Yield: 67%. $^{1}$H NMR (400 MHz, $CDCl_3$) δ 2.22 (3H, s), 2.72 (3H, s), 2.97 (1H, dd, *J* = 4.4, 11.2 Hz), 3.40-3.44 (1H, m), 3.50 (1H, dd, *J* = 2.8, 11.6 Hz), 4.02 (1H, d, *J* = 9.6 Hz), 6.57 (1H, d, *J* = 8.4 Hz), 6.95 (1H, dd, *J* = 1.6, 8.4 Hz), 7.17-7.20 (2H, m), 7.32-7.36 (2H, m); $^{13}$C NMR (100 MHz, $CDCl_3$) δ = 20.4, 39.6, 42.1, 43.5, 50.9, 112.6, 118.5, 126.3, 128.4, 128.9, 129.0, 129.2, 130.8, 132.0, 146.2, 175.8, 177.8.

**8-Fluoro-5-methyl-2-phenyl-3a,4,5,9b-tetrahydro-1*H*-pyrrolo[3,4-*c*]quinoline-1,3(2*H*)-dione (5h)**

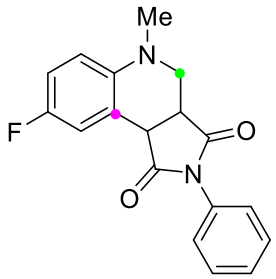


NMR Yield: 73%. $^{1}$H NMR (400 MHz, $CDCl_3$) δ 2.84 (3H, s), 3.11 (1H, dd, *J* = 4.4, 11.2 Hz), 3.54-3.63 (2H, m), 4.14 (1H, d, *J* = 9.6 Hz), 6.71 (1H, dd, *J* = 4.8, 8.8 Hz), 6.97 (1H, ddd, *J* = 2.8, 6.0, 14.4 Hz), 7.11-7.18 (1H, m), 7.28-7.32 (3H, m), 7.44-7.48 (2H, m); $^{13}$C NMR (100 MHz, $CDCl_3$) δ = 39.8, 42.1, 43.3, 51.0, 113.5 (d, *J* = 7.5 Hz), 115.1 (d, *J* = 21.9 Hz), 116.5 (d, *J* = 22.6 Hz), 117.0 (d, *J* = 23.3 Hz), 120.1 (d, *J* = 7.7 Hz), 126.3, 128.6, 129.0, 131.8, 144.8 (d, *J* = 1.9 Hz), 156.7 (d, *J* = 237.7 Hz), 175.1, 177.4.

**5-Ethyl-2-phenyl-3a,4,5,9b-tetrahydro-1*H*-pyrrolo[3,4-*c*]quinoline-1,3(2*H*)-dione (5i)**

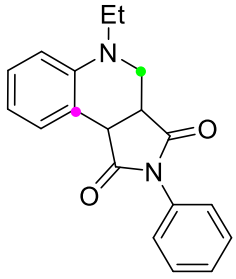


NMR Yield: 73%. $^{1}$H NMR (400 MHz, $CDCl_3$) δ 1.11 (3H, t, *J* = 7.2 Hz), 3.11 (1H, dd, *J* = 4.0, 11.6 Hz), 3.15-3.31 (2H, m), 3.46-3.50 (1H, m), 3.58 (1H, dd, *J* = 2.8, 11.6 Hz), 4.07 (1H, d, *J* = 9.6 Hz), 6.71 (1H, d, *J* = 8.0 Hz), 6.79 (1H, t, *J* = 7.2 Hz), 7.12-7.19 (3H, m), 7.28 (1H, dd, *J* = 7.2, 7.6 Hz), 7.36 (2H, dd, *J* = 7.2, 8.0 Hz), 7.45 (1H, d, *J* = 7.6 Hz); $^{13}$C NMR (100 MHz, $CDCl_3$) δ = 10.8, 42.3, 43.8, 44.9, 47.1, 112.8, 118.6, 119.2, 126.3, 128.5, 128.6, 129.0, 130.7, 132.0, 146.9, 175.8, 177.7.

Table S4. Representative heterogeneous porous catalysts for the oxidative coupling of tertiary anilines with maleimides.

| Catalyst | Reaction conditions | Yield | Reference |
|---|---|---|---|

| | | | |
|---|---|---|---|
| $Ru(bpy)_3$@NKMOF-4 | 0.5 mmol [T], 0.25 mmol [M], 3 mol % [P], 3.0 mL DMF, two 23 W CFL, r.t., 36 h | 71% | 17 |
| P-BBT-10 | 0.5 mmol [T], 0.25 mmol [M], 10 mg [P], 3.0 mL DMF, white LED, r.t., air, 24 h. | 67% | 18 |
| $H_2P$-Bph-COF | 0.2 mmol [T], 0.1 mmol [M], 8 mol% [P], 3 mL $CHCl_3$, blue LEDs (λ= 450 nm), r.t., $O_2$, 14 h | 72% | 19 |
| UiO-68-TDP | 0.2 mmol [T], 0.1 mmol [M], 4 mg [P], 1 mL $CH_3CN$, blue LED, air, r.t., 12 h | 82% | 20 |
| JNU-204 | 0.5 mmol [T], 0.25 mmol [M], 1mol% [P], 5mL DMF, blue LED, air, r.t., 48h | 75% | This work |
| JNU-207 | 0.5 mmol [T], 0.25 mmol [M], 1mol% [P], 5mL DMF, blue LED, air, r.t., 48h | 77% | This work |

[T] = tertiary anilines; [M] = maleimides; [P] = photocatalyst; r.t. = room temparture.

### 3.3 Photocatalytic reaction mechanisms verification

We performed the photocatalytic synthesis of imines in the presence of a known $O_2^{\bullet-}$ quencher, *p*-benzoquinone (BQ). As shown below, the significantly reduced yield of **2a** indicates that $O_2^{\bullet-}$ is key intermediate in this reaction.

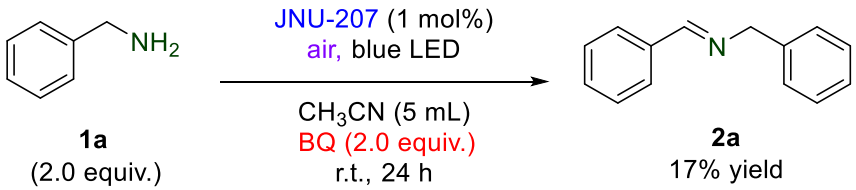


Fig. S16. Mechanistic studies of the photocatalytic synthesis of imines.

We performed the photocatalytic synthesis of tetrahydroquinoline derivatives in the presence of a known $O_2^{\bullet-}$ quencher, *p*-benzoquinone (BQ). As shown below, the significantly reduced yield of **5a** indicates that $O_2^{\bullet-}$ is key intermediate in this reaction.

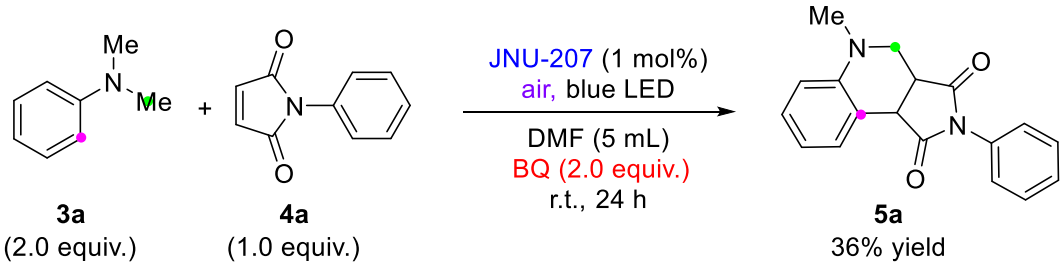


Fig. S17. Mechanistic studies of the photocatalytic synthesis of tetrahydroquinoline

derivatives.

## Section 4. Recycling experiments

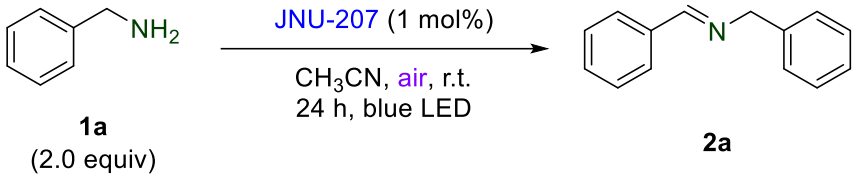


According to the general procedure **A**, 10 parallel reactions were carried out at the same time. After the reaction completion, **JNU-207** was recovered by centrifugation, one of them was used to detect the yield by NMR, and the rest were all centrifuged, washed with acetonitrile and dried. Following the above reaction condition, the second cycle and third cycle of this reaction was performed, and **2a** could be assembled in 94% yield and 92% yield, respectively. The resulting powder J**NU-207** was used for other characterizations.

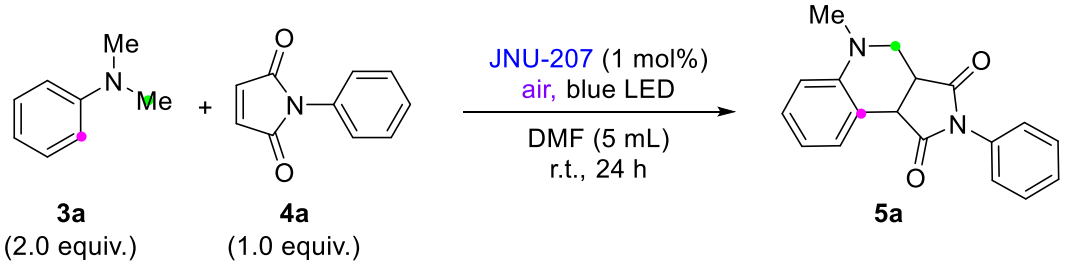


According to the general procedure **B**, 10 parallel reactions were carried out at the same time. After the reaction completion, **JNU-207** was recovered by centrifugation, one of them was used to detect the yield by NMR, and the rest were all centrifuged, washed with acetonitrile and dried. Following the above reaction condition, the second cycle and third cycle of this reaction was performed, and **5a** could be assembled in 76% yield and 76% yield, respectively.

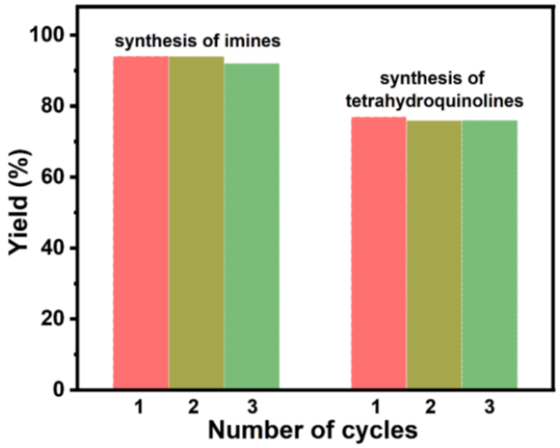


Fig. S18. Recycling experiments with **JNU-207** as the photocatalyst for synthesis of imines and synthesis of tetrahydroquinolines (the three cycles are light red, dark yellow, and olive, respectively).

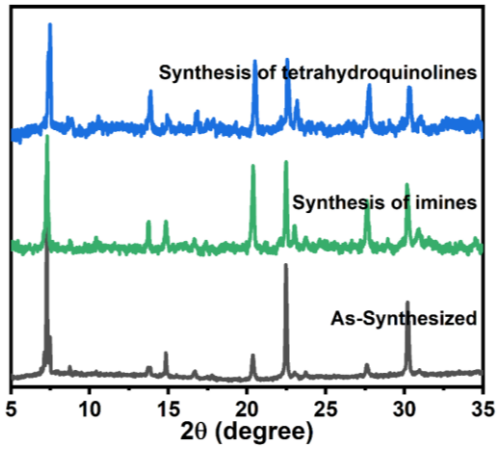


Fig. S19. Comparison of PXRD patterns of the pristine **JNU-207** and the recovered **JNU-207** after three runs of each experiment (three reactions)

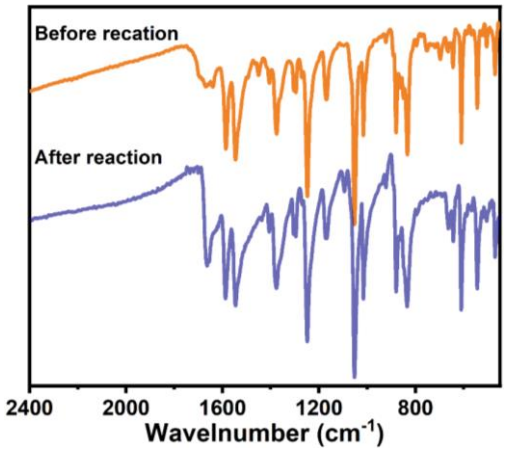


Fig. S20. FT-IR spectra of **JNU-207** before and after photocatalytic synthesis of (*E*)-N-benzyl-1-phenylmethanimine.

**Table S5**. ICP-AES results[a] for **JNU-207** after photocatalytic oxidation of benzylamine.

| | *ρ*(Co) / ppm |
|---|---|
| 1 | 2.149 |
| 2 | 1.098 |
| 3 | 2.253 |

## Section 5. Reference


1. J. K. Jin, K. Wu, X. Y. Liu, G. Q. Huang, Y. L. Huang, D. Luo, M. Xie, Y. Zhao, W. Lu, X. P. Zhou, J. He and D. Li, *J. Am. Chem. Soc.*, 2021, **143**, 21340–21349.
2. C. Wang, Z. Xie, K. E. deKrafft and W. Lin, *J. Am. Chem. Soc.*, 2011, **133**, 13445–13454.
3. D. Sun, L. Ye and Z. Li, *Appl. Catal. B-Environ.*, 2015, **164**, 428–432.
4. C. Xu, H. Liu, D. Li, J. H. Su and H. L. Jiang, *Chem. Sci.*, 2018, **9**, 3152–3158.
5. J. A. Johnson, J. Luo, X. Zhang, Y.-S. Chen, M. D. Morton, E. Echeverría, F. E. Torres and J. Zhang, *ACS Catal.*, 2015, **5**, 5283–5291.
6. L. Zeng, T. Liu, C. He, D. Shi, F. Zhang and C. Duan, *J. Am. Chem. Soc.*, 2016, **138**, 3958–3961.
7. H. Wei, Z. Guo, X. Liang, P. Chen, H. Liu and H. Xing, *ACS Appl. Mater. Interfaces*, 2019, **11**, 3016–3023.

8. J. Shi, J. Zhang, T. Liang, D. Tan, X. Tan, Q. Wan, X. Cheng, B. Zhang, B. Han, L. Liu, F. Zhang and G. Chen, *ACS Appl. Mater. Interfaces*, 2019, **11**, 30953–30958.
9. Z. X. Sun, K. Sun, M. L. Gao, O. Metin and H. L. Jiang, *Angew. Chem. Int. Ed.*, 2022, e202206108.
10. M. H. Li, Z. Q. Yang, Z. Li, J. R. Wu, B. Yang and Y. W. Yang, *Chem. Mater.*, 2022, **34**, 5726–5739.
11. Z. Liu, X. Li, J. Chen, C. Li, F. Luo, F. X. Cheng and J. J. Liu, *Dalton. Trans.*, 2022, **51**, 8472–8479.
12. L. M. Aguirre-Diaz, N. Snejko, M. Iglesias, F. Sanchez, E. Gutierrez-Puebla and M. A. Monge, *Inorg. Chem.*, 2018, **57**, 6883–6892.
13. H. Li, Y. Yang, C. He, L. Zeng and C. Duan, *ACS Catal.*, 2018, **9**, 422–430.
14. T. Wu, Y. Shi, Z. Wang, C. Liu, J. Bi, Y. Yu and L. Wu, *ACS Appl. Mater. Interfaces*, 2021, **13**, 61286–61295.
15. F. J. Zhao, G. Zhang, Z. Ju, Y. X. Tan and D. Yuan, *Inorg. Chem.*, 2020, **59**, 3297–3303.
16. Z. Liu, C. Li, J. Chen, X. Li, F. Luo, F. Cheng and J.-J. Liu, *Inorg. Chem. Front.*, 2022, **9**, 111–118.
17. X. Yang, T. Liang, J. Sun, M. J. Zaworotko, Y. Chen, P. Cheng and Z. Zhang, *ACS Catal.*, 2019, **9**, 7486–7493.
18. Z. J. Wang, S. Ghasimi, K. Landfester and K. A. I. Zhang, *Adv. Synth. Catal.*, 2016, **358**, 2576–2582.
19. C. Wu, X. Li, M. Shao, J. Kan, G. Wang, Y. Geng and Y.-B. Dong, *Chin. Chem. Lett.*, 2022, **33**, 4559–4562.
20. C. Li, H. Zhang, X. Wang, Q. Y. Li, X. Zhao and X. J. Wang, *RSC Adv.*, 2022, **12**, 1638–1644.

## Appendix

$^{1}H$ and $^{13}C$ NMR spectra for new compounds.

$^{1}$H NMR (400 MHz, $CDCl_3$) spectrum of **2a**

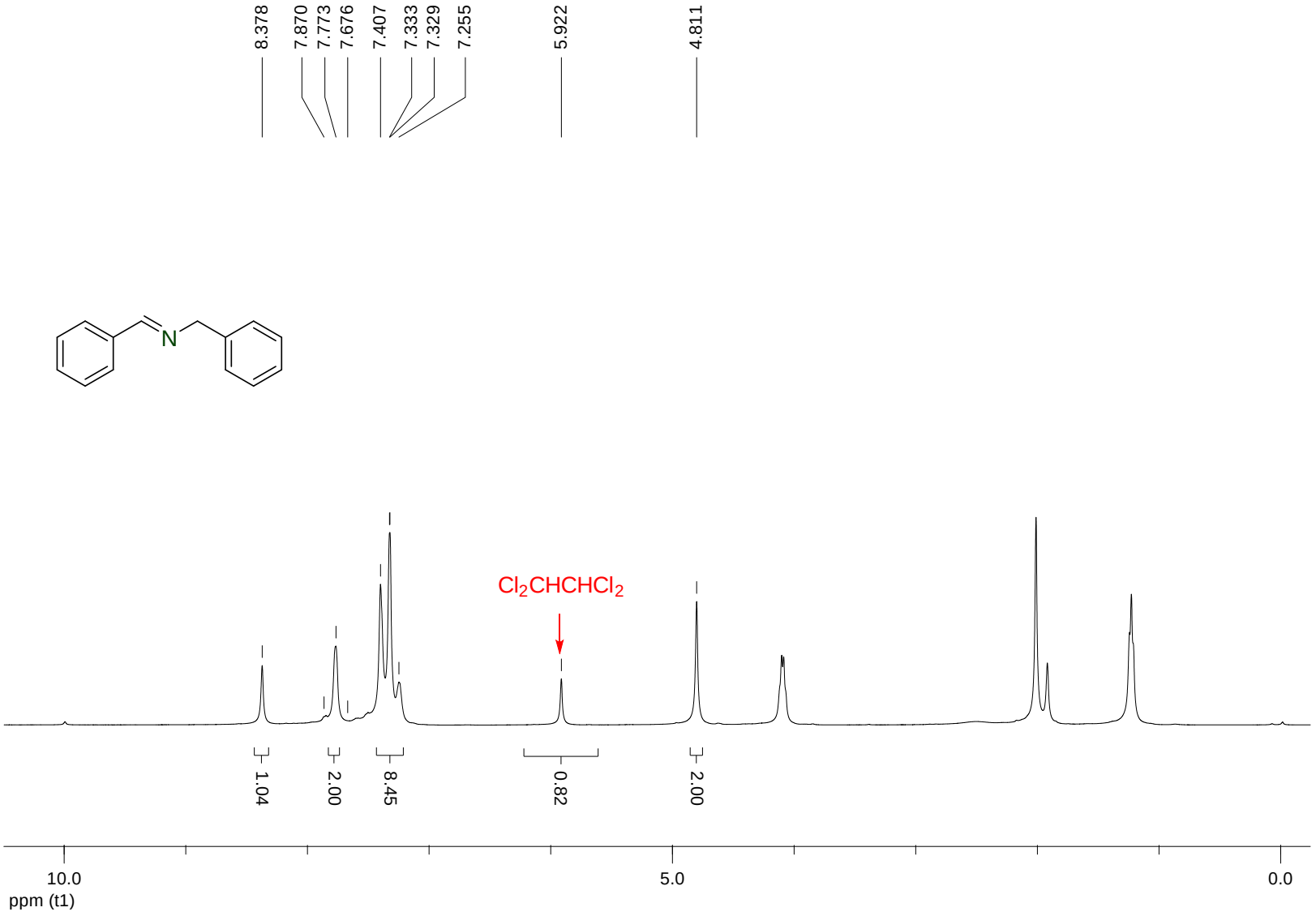

$^{1}$H NMR (400 MHz, $CDCl_3$) spectrum of **2b**

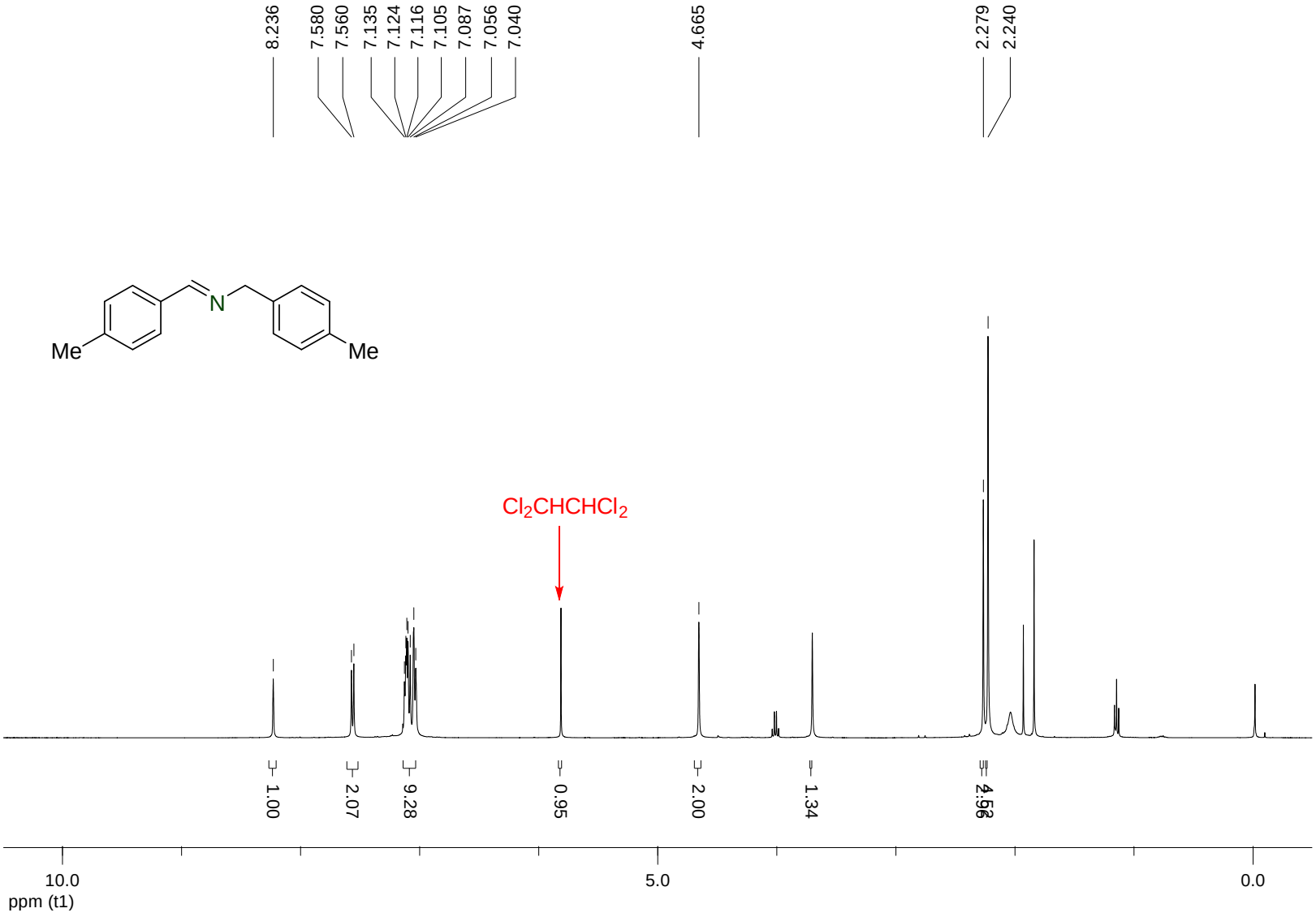

$^{1}$H NMR (400 MHz, $CDCl_3$) spectrum of **2c**

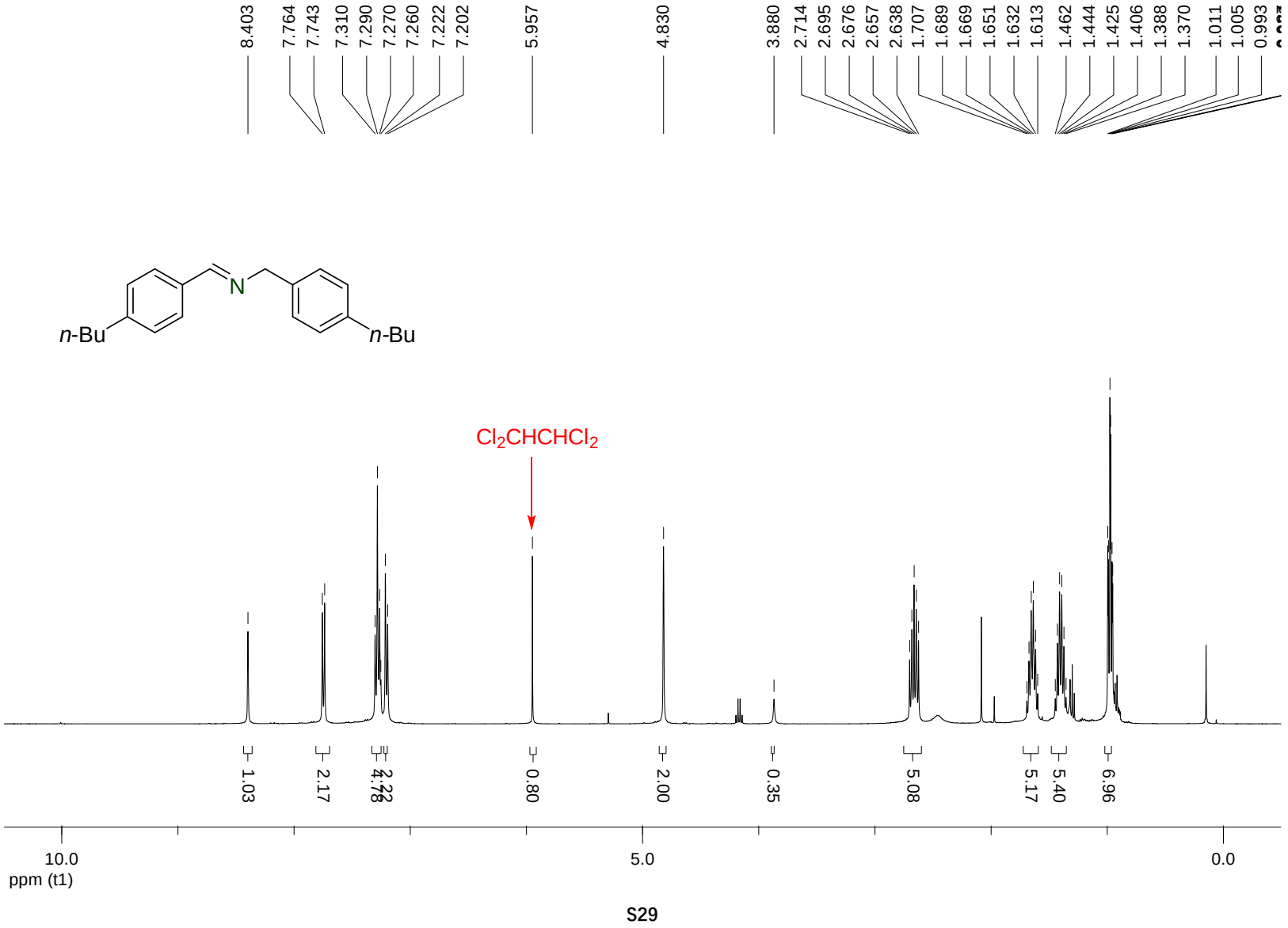

$^{1}$H NMR (400 MHz, $CDCl_3$) spectrum of **2d**

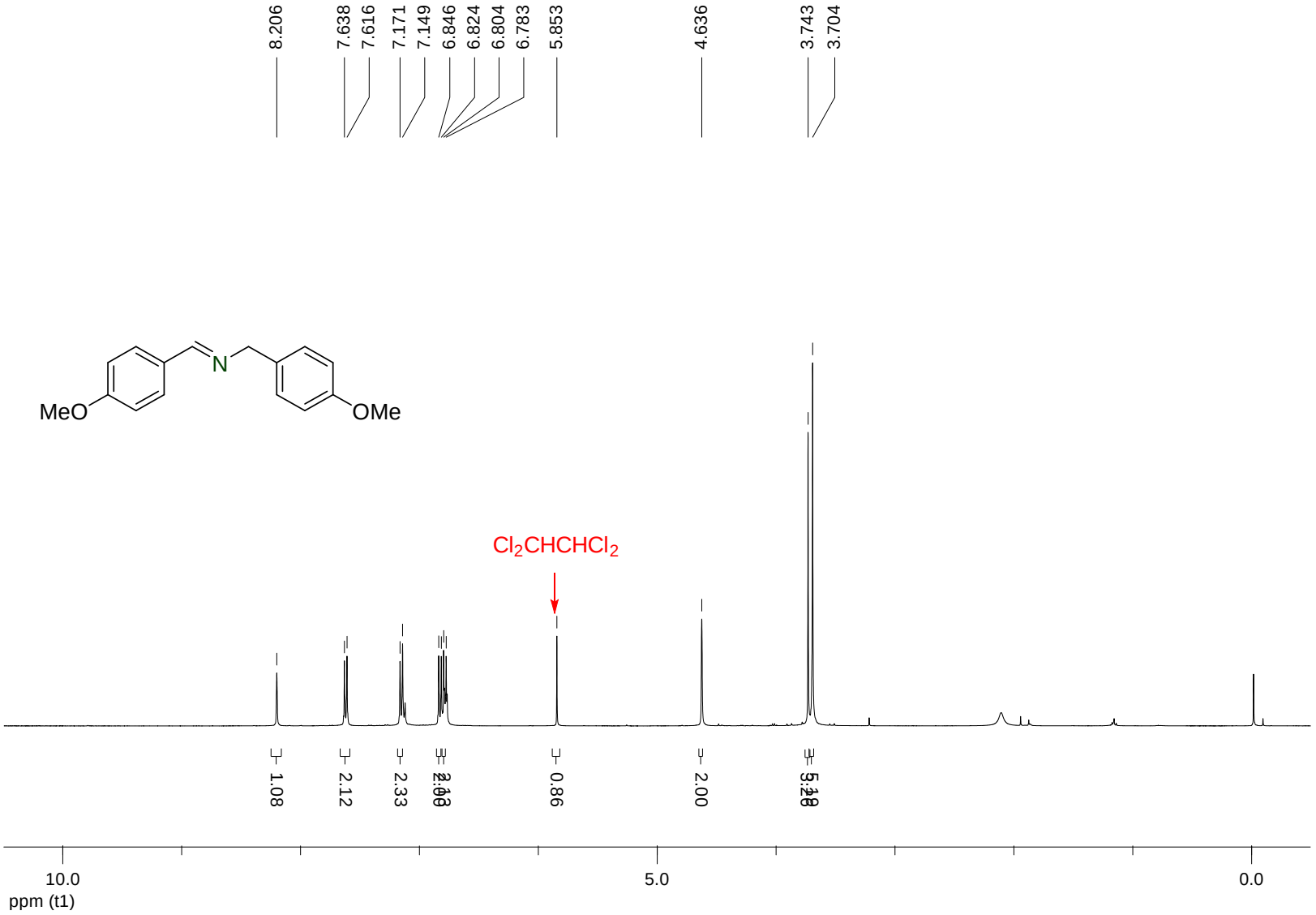

$^{1}$H NMR (400 MHz, $CDCl_3$) spectrum of **2e**

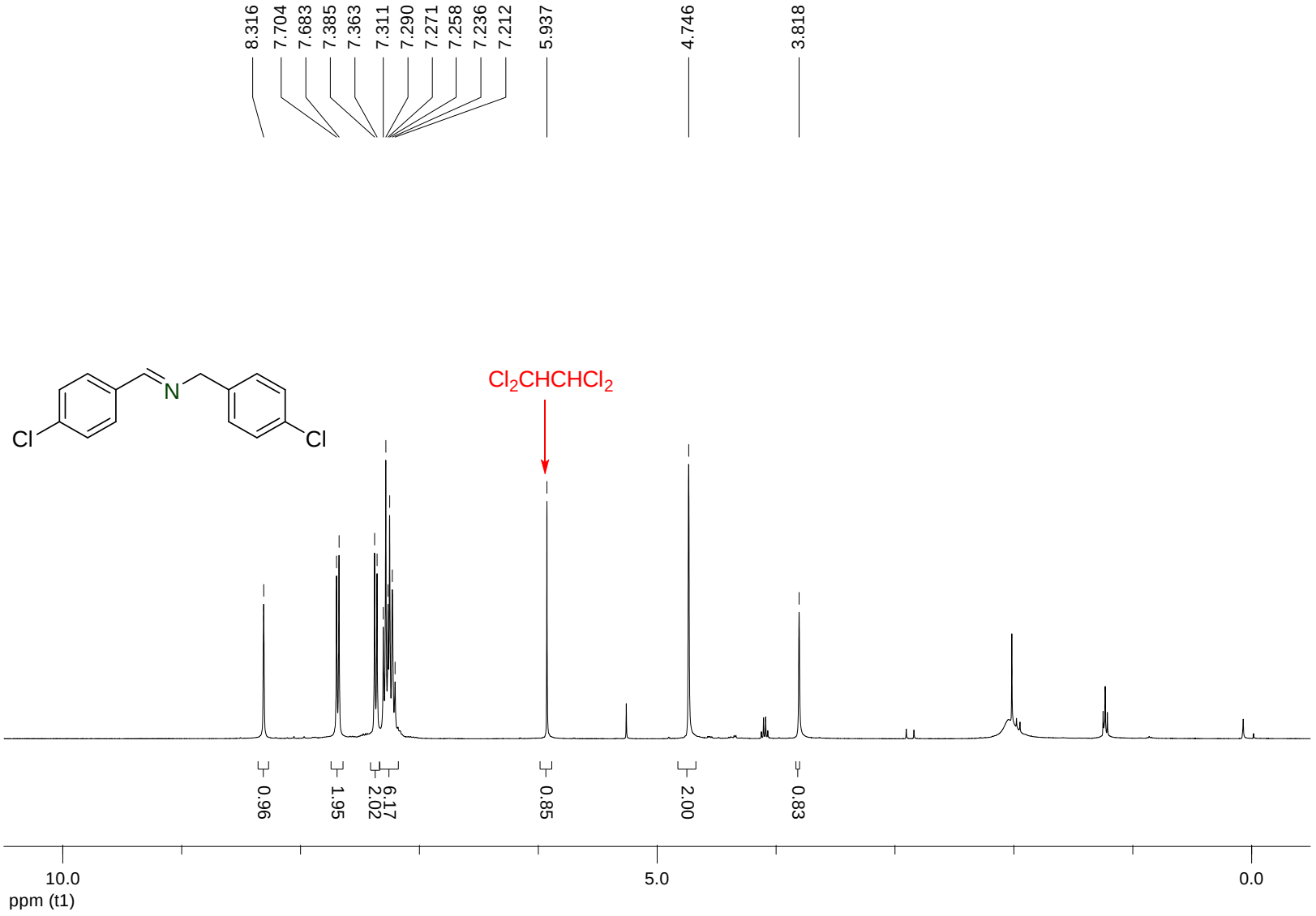

$^{1}$H NMR (400 MHz, $CDCl_3$) spectrum of **2f**

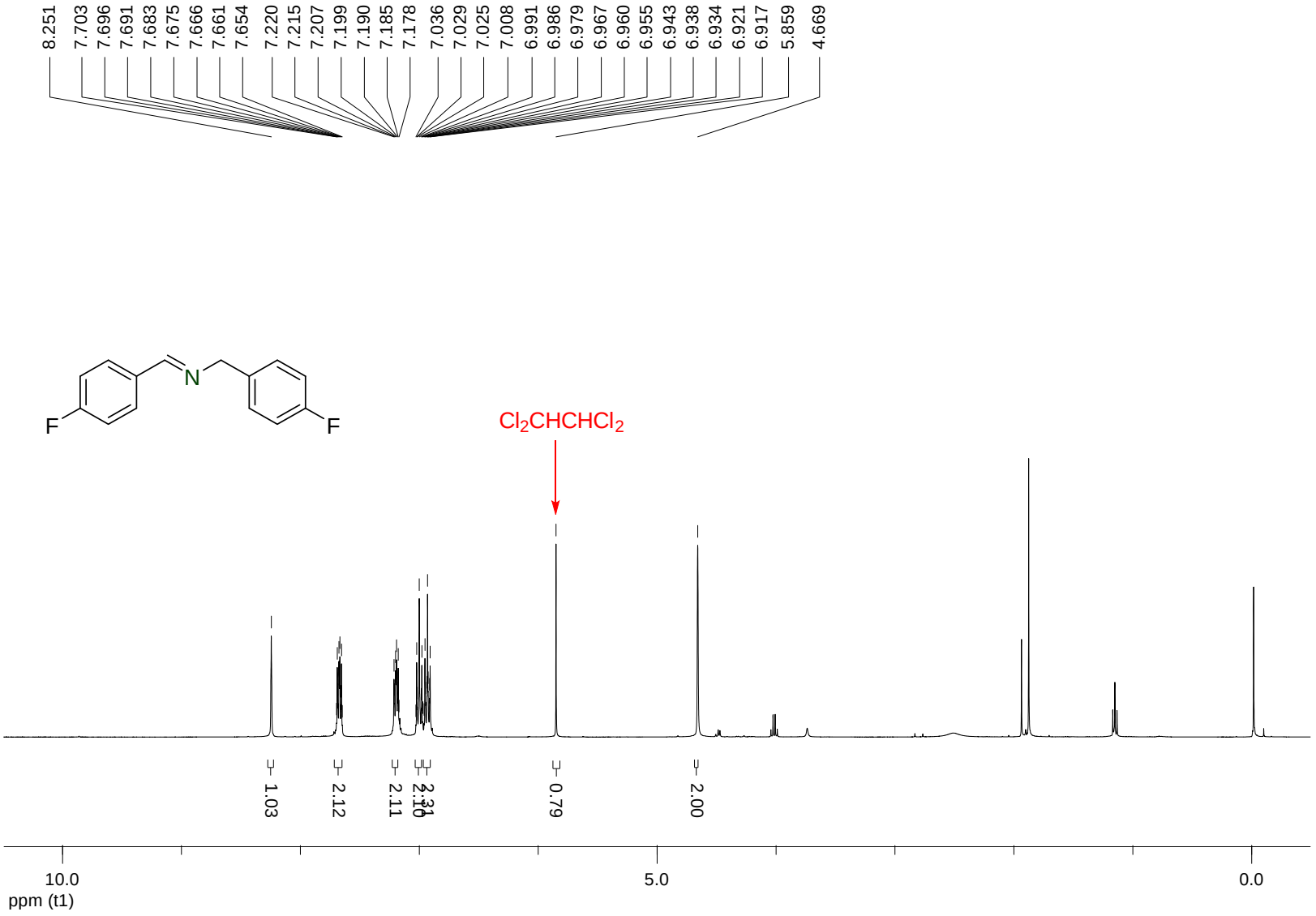

$^{1}$H NMR (400 MHz, $CDCl_3$) spectrum of **2g**

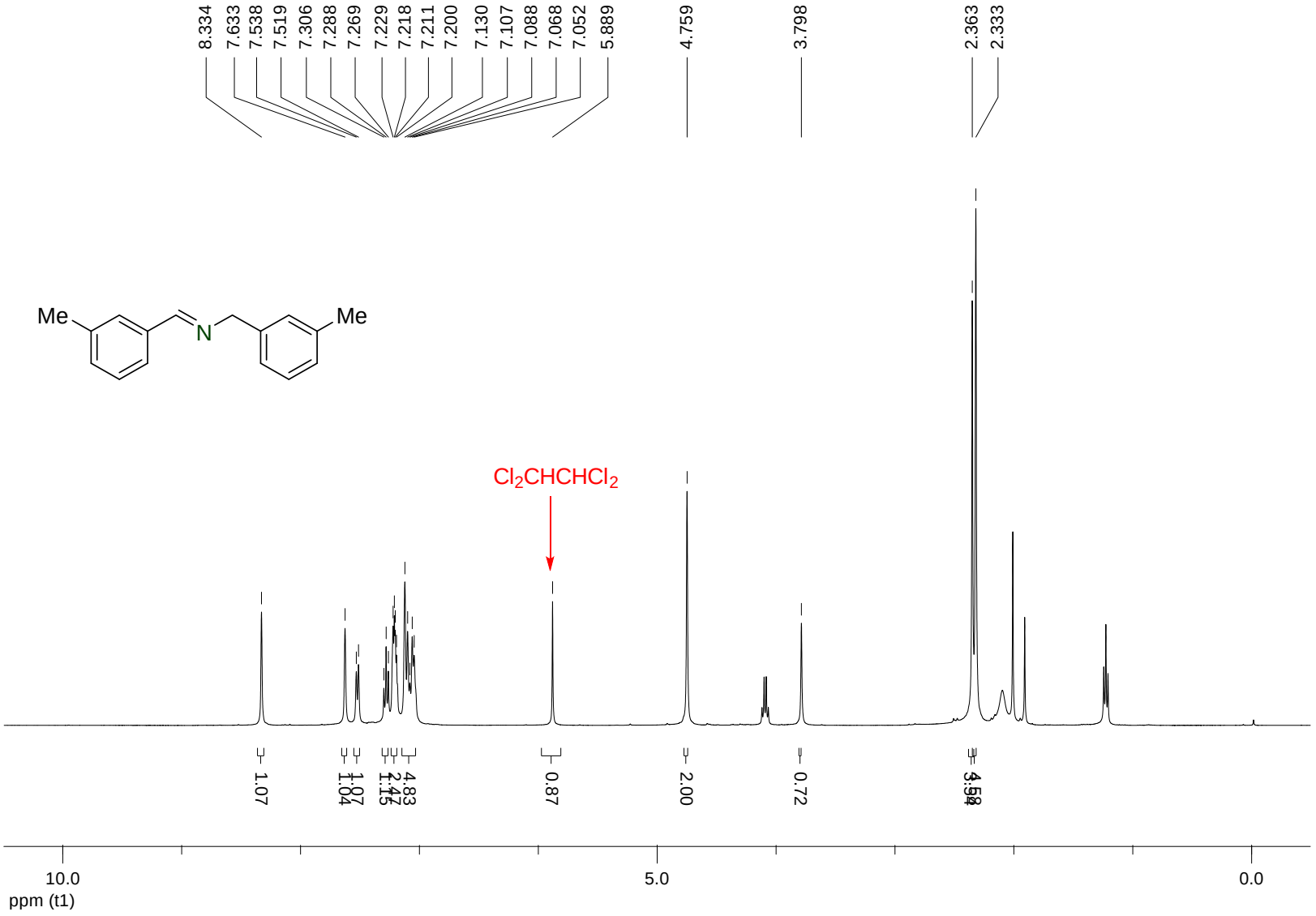

$^{1}$H NMR (400 MHz, $CDCl_3$) spectrum of **2h**

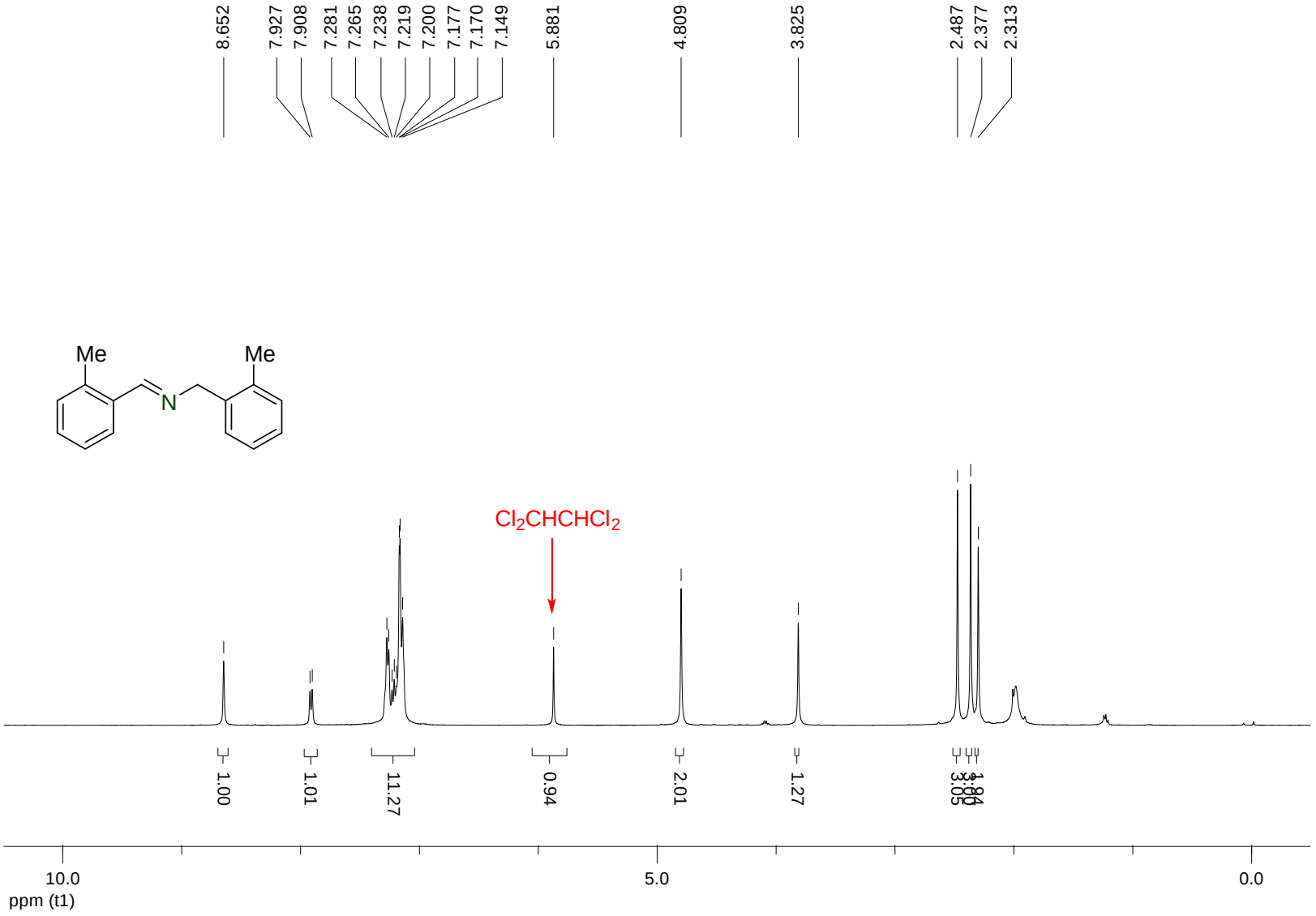

$^{1}$H NMR (400 MHz, $CDCl_3$) spectrum of **5a**

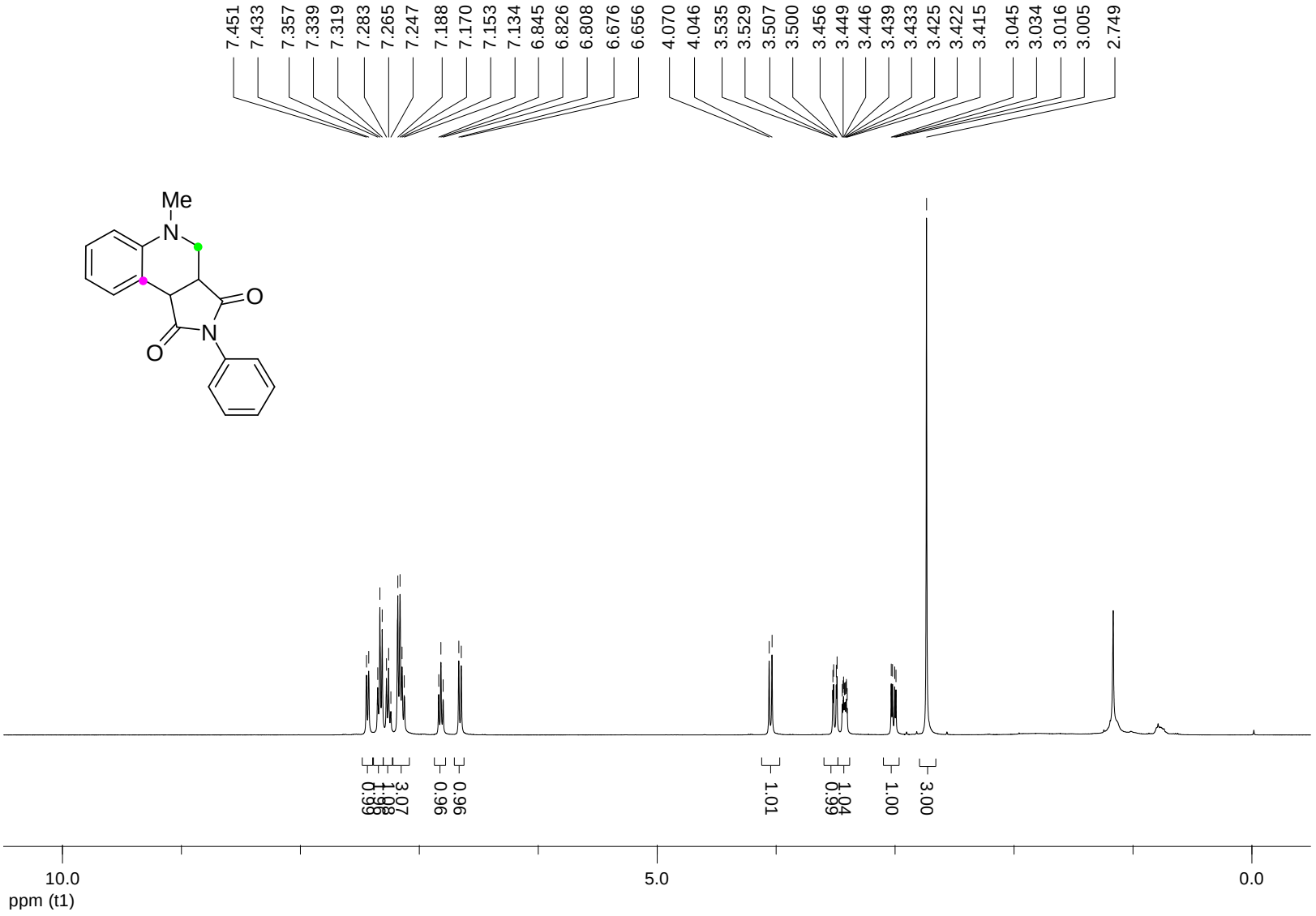

$^{13}$C NMR (100 MHz, $CDCl_3$) spectrum of **5a**

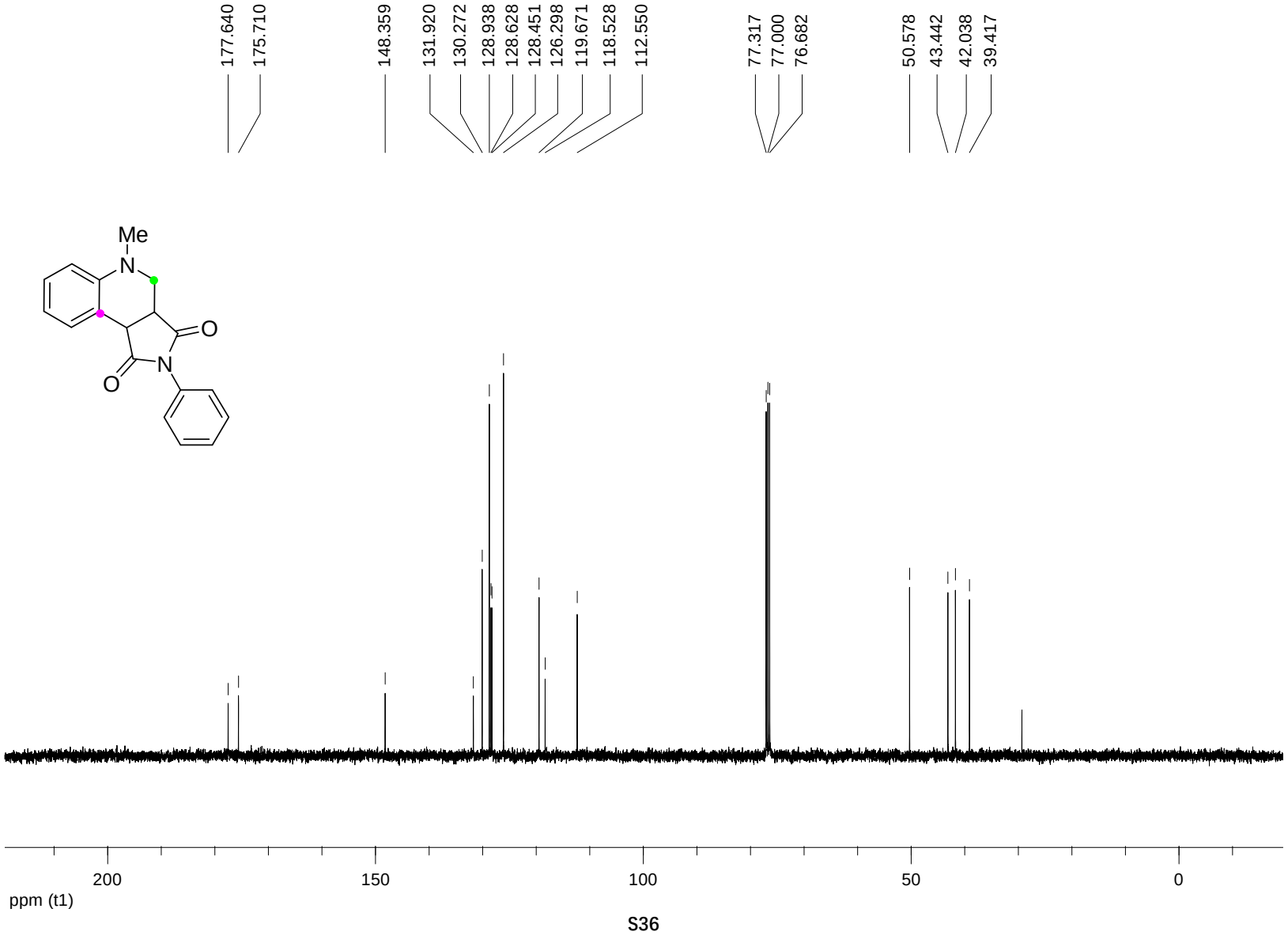

$^{1}$H NMR (400 MHz, $CDCl_3$) spectrum of **5b**

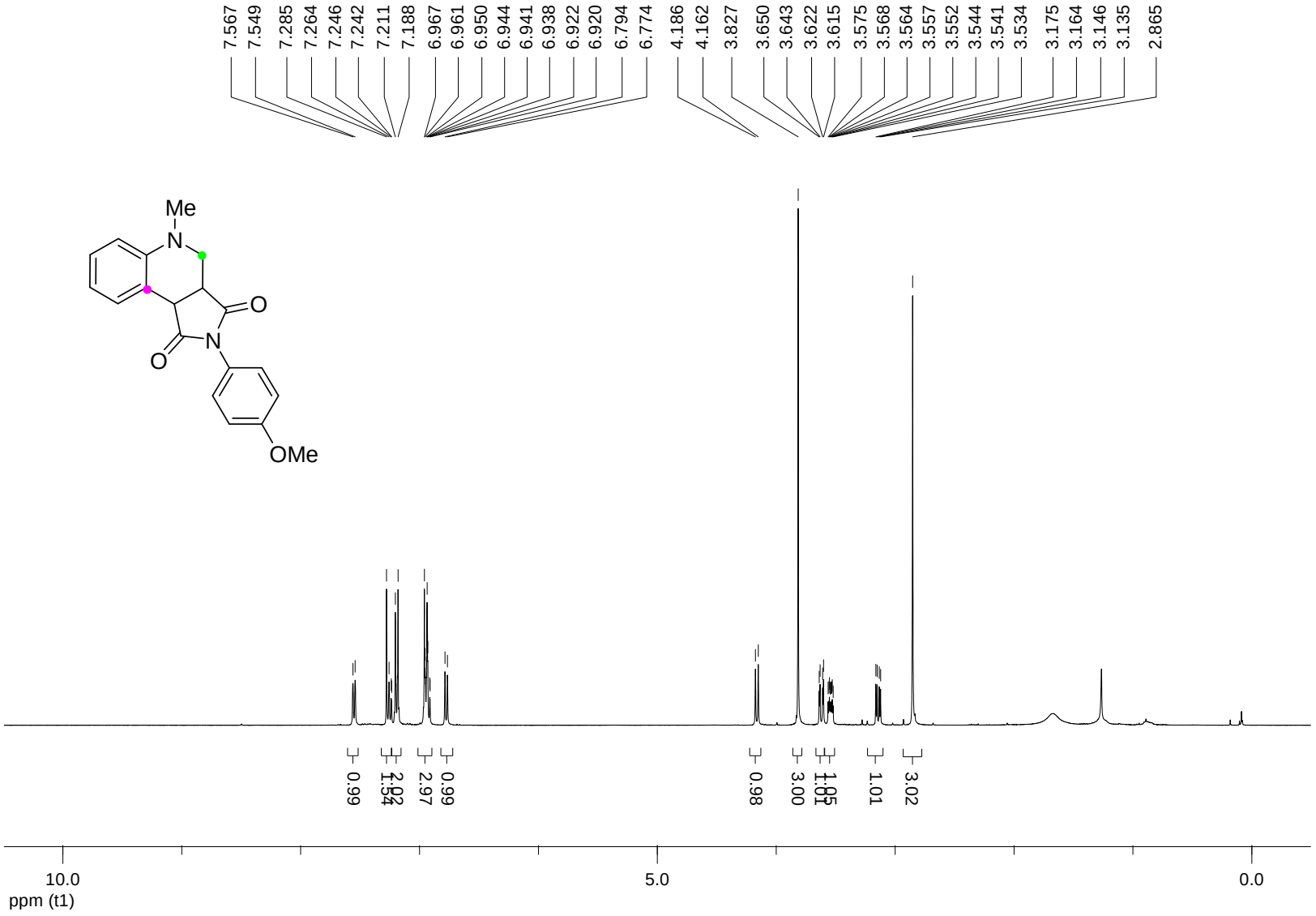

$^{13}C$ NMR (100 MHz, $CDCl_3$) spectrum of **5b**

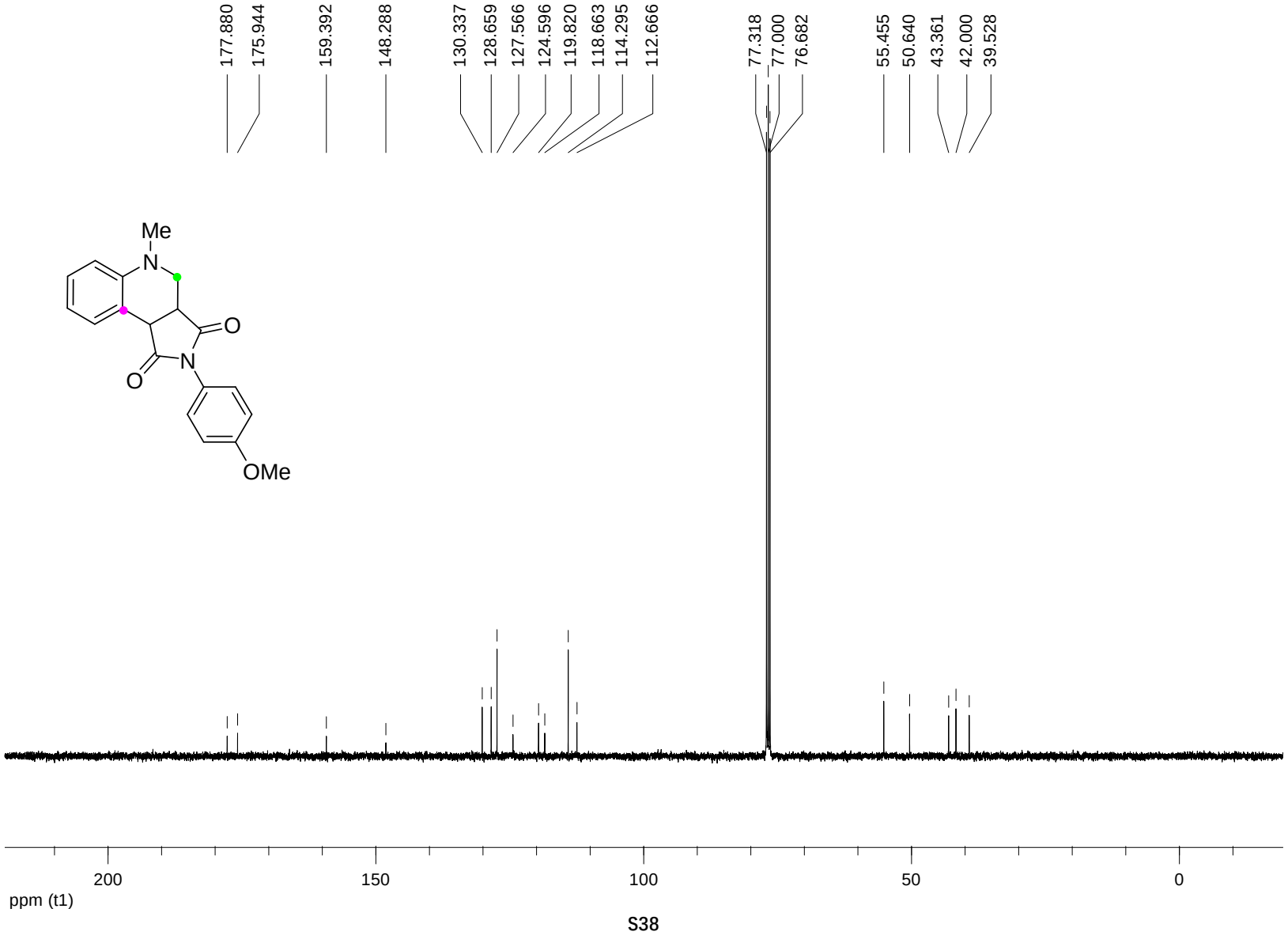

$^{1}$H NMR (400 MHz, $CDCl_3$) spectrum of **5c**

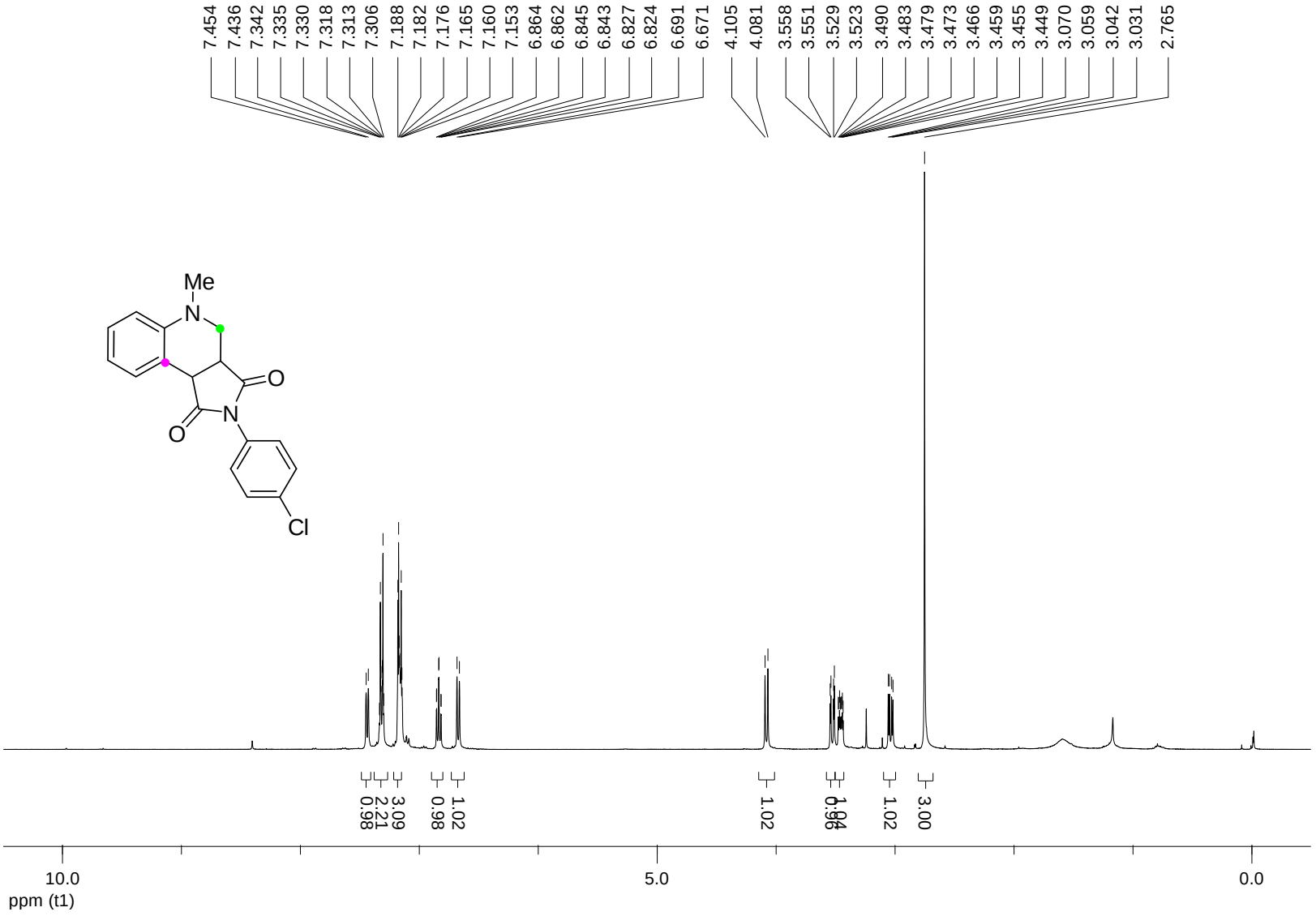

$^{13}$C NMR (100 MHz, $CDCl_3$) spectrum of **5c**

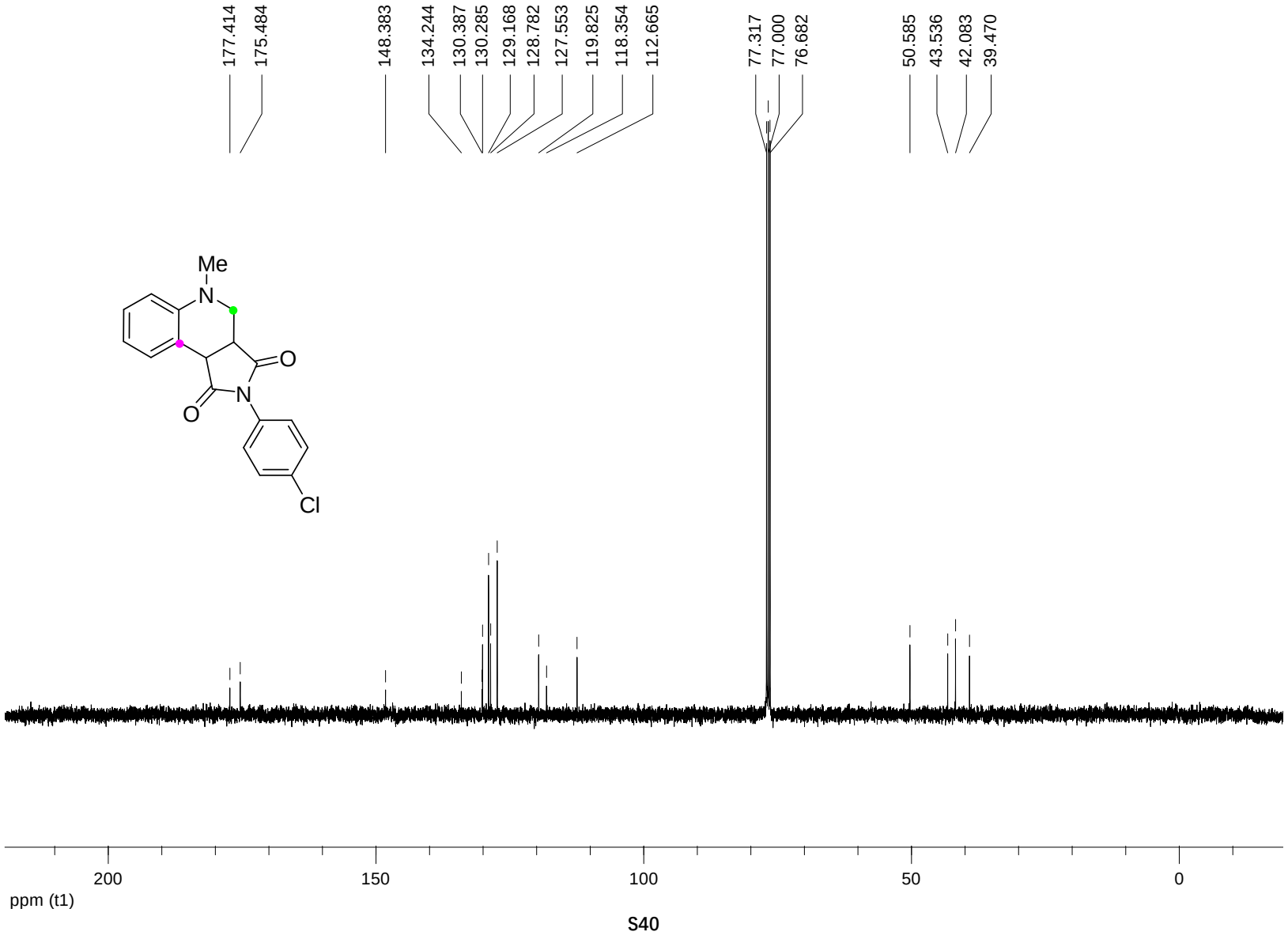

$^{1}$H NMR (400 MHz, $CDCl_3$) spectrum of **5d**

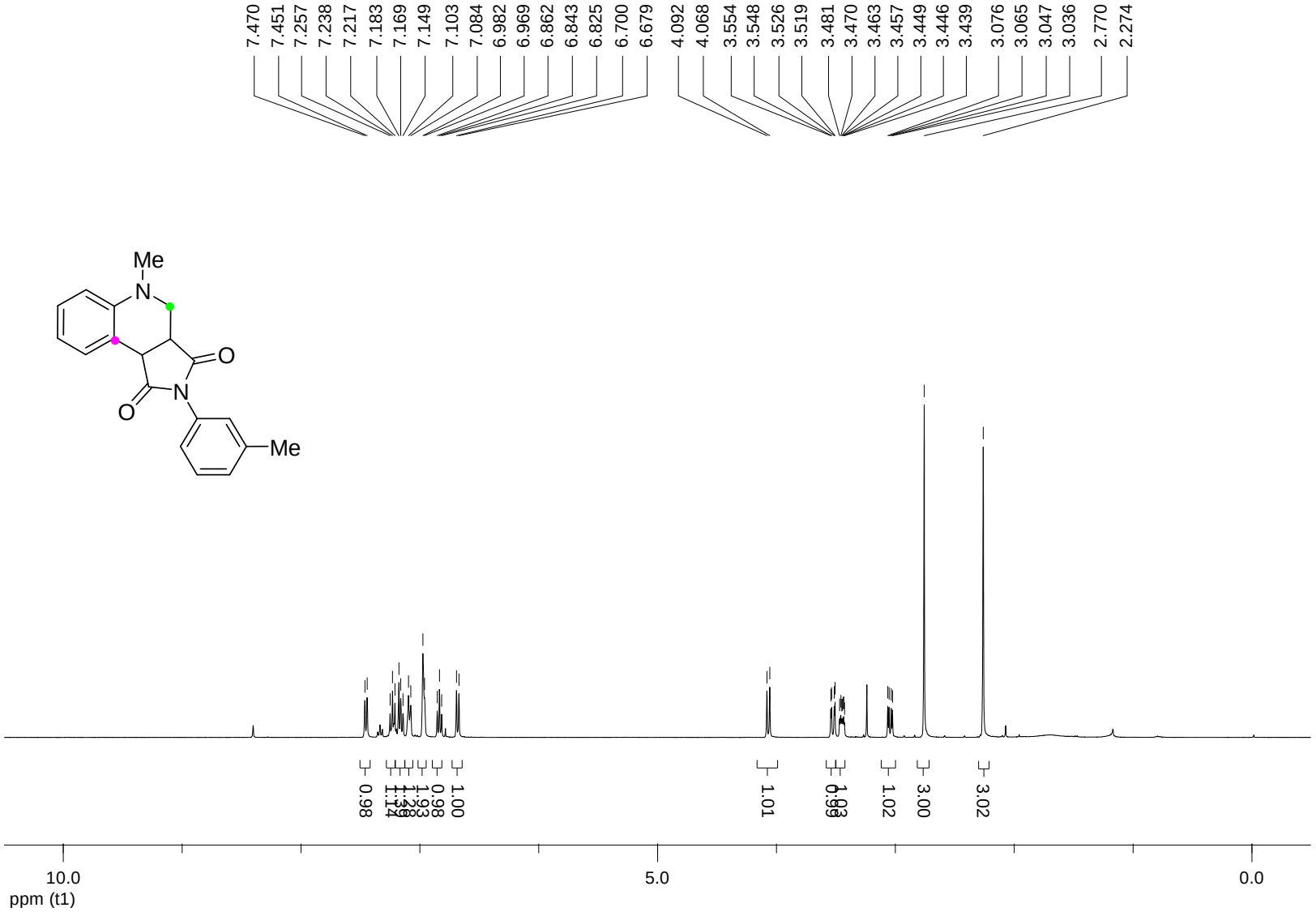

$^{13}C$ NMR (100 MHz, $CDCl_3$) spectrum of **5d**

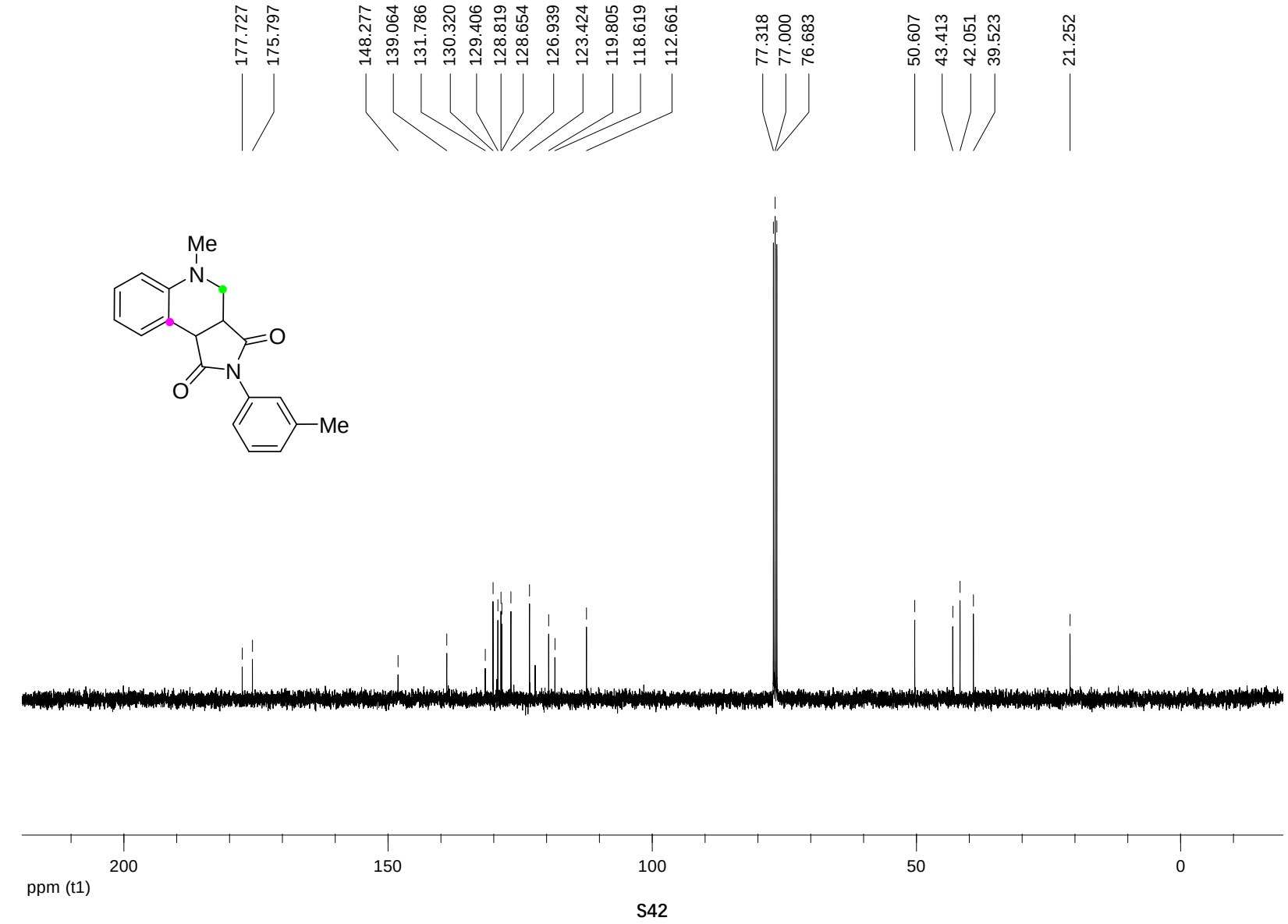

$^{1}$H NMR (400 MHz, $CDCl_3$) spectrum of **5e**

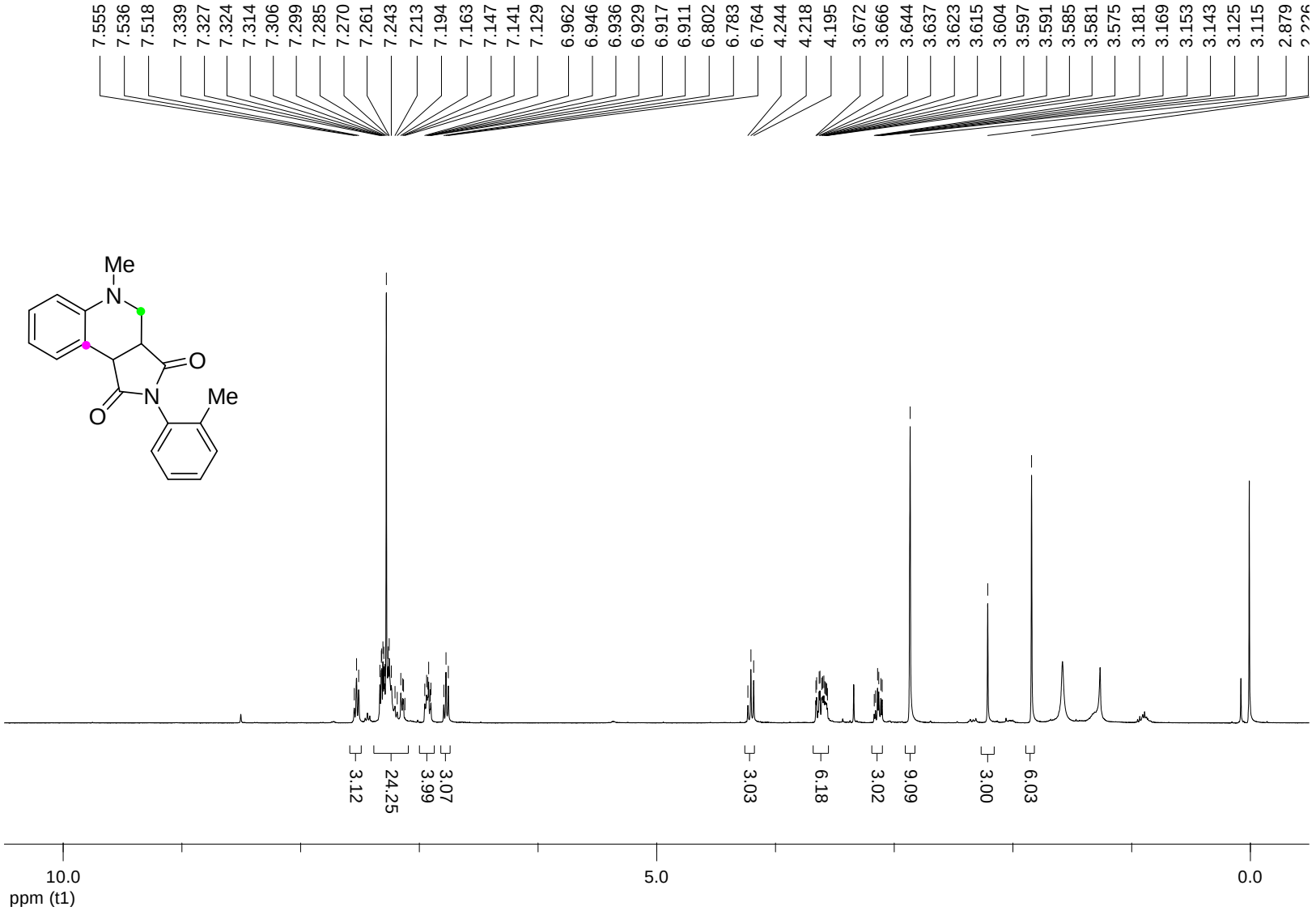

$^{13}C$ NMR (100 MHz, $CDCl_3$) spectrum of **5e**

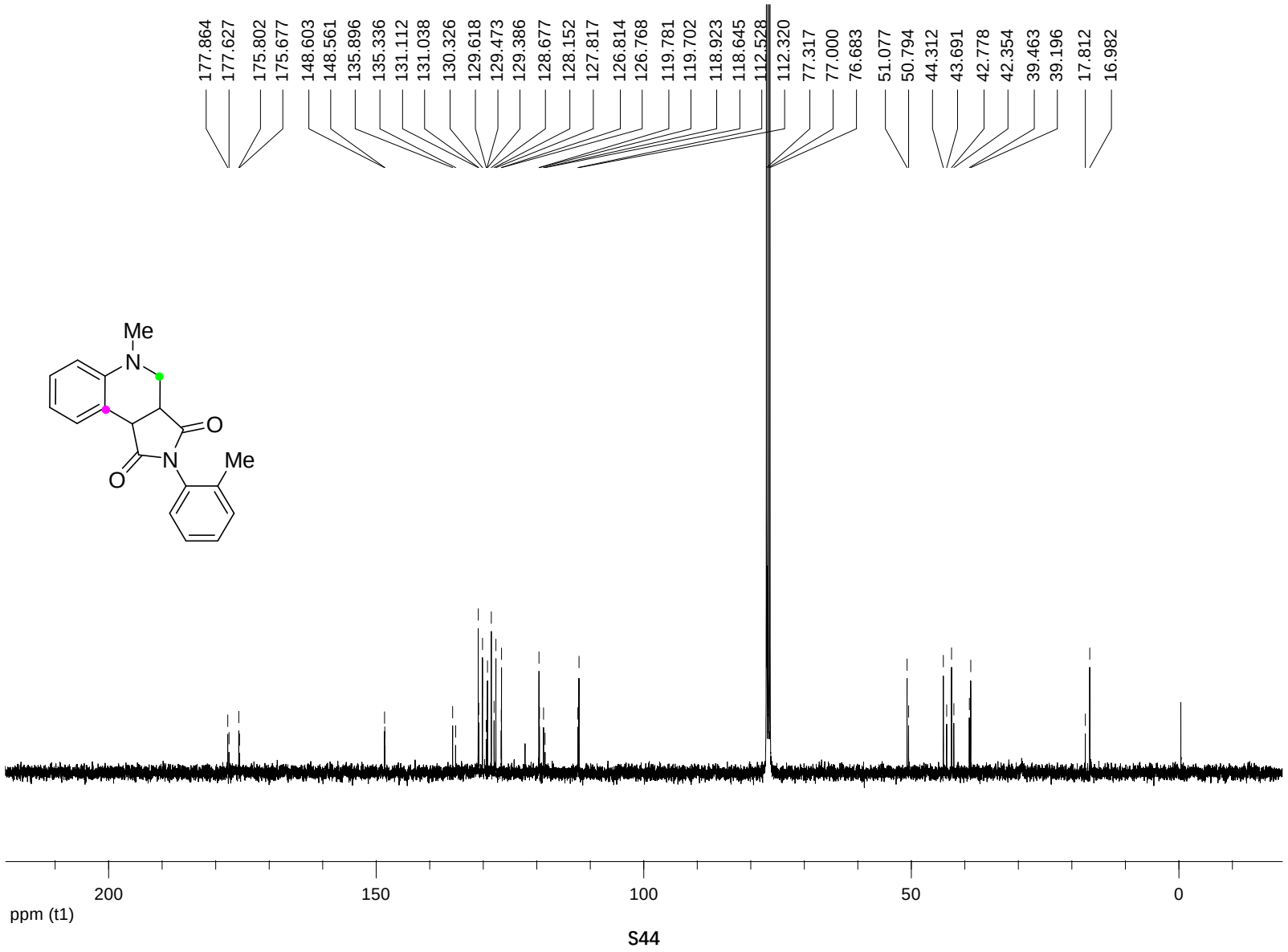

$^{1}$H NMR (400 MHz, $CDCl_3$) spectrum of **5f**

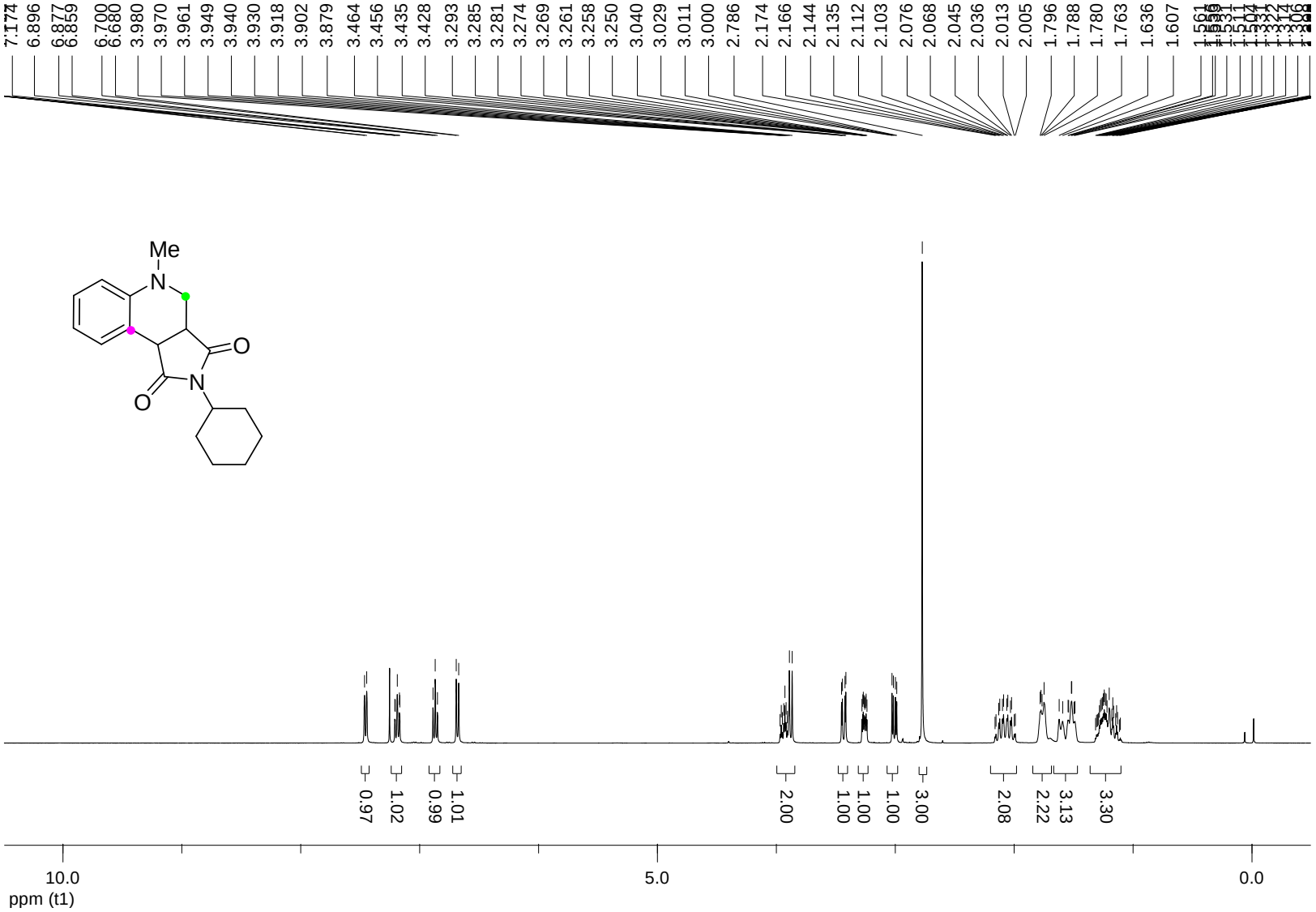

$^{13}$C NMR (100 MHz, $CDCl_3$) spectrum of **5f**

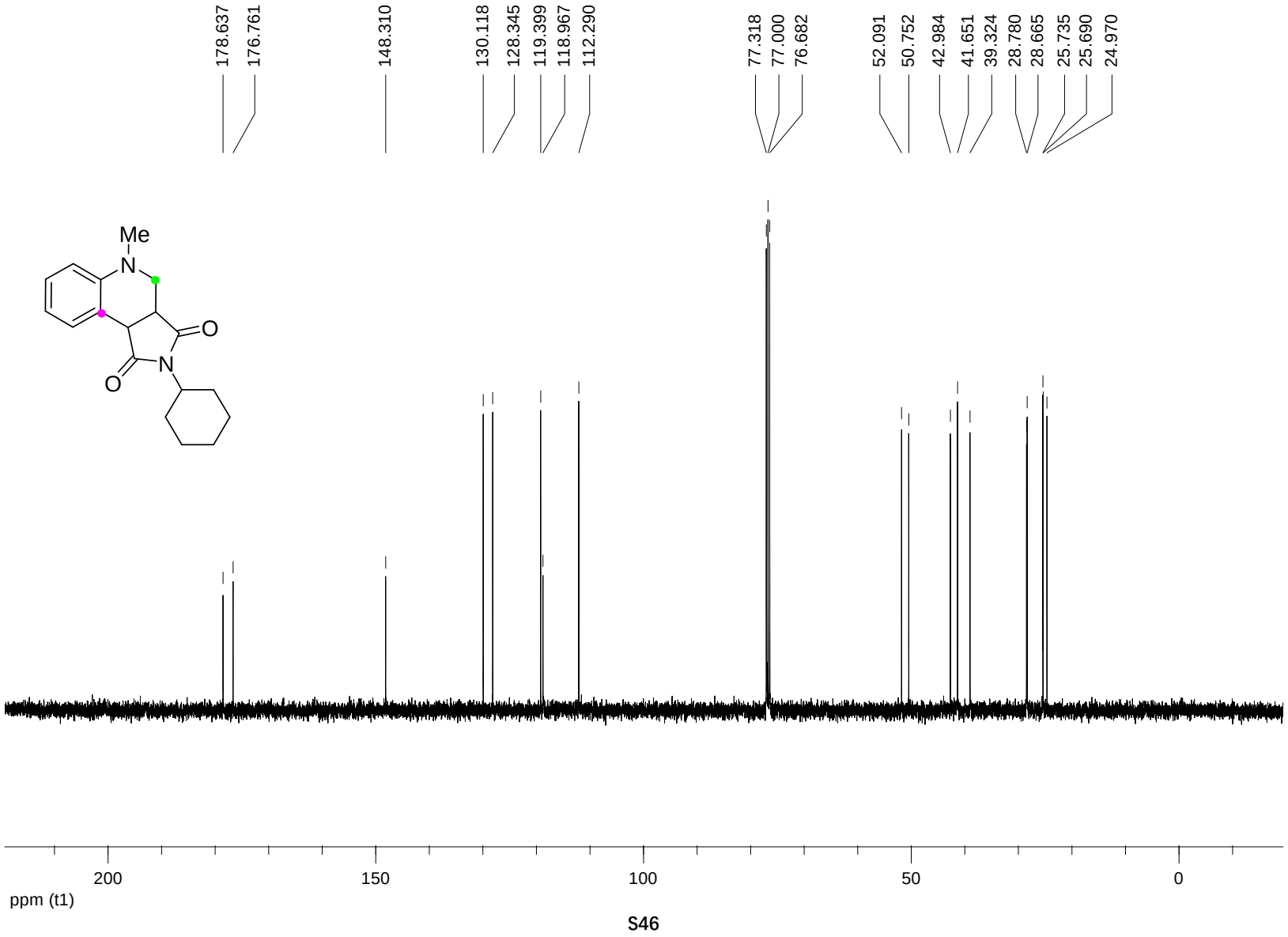

$^{1}$H NMR (400 MHz, $CDCl_3$) spectrum of **5g**

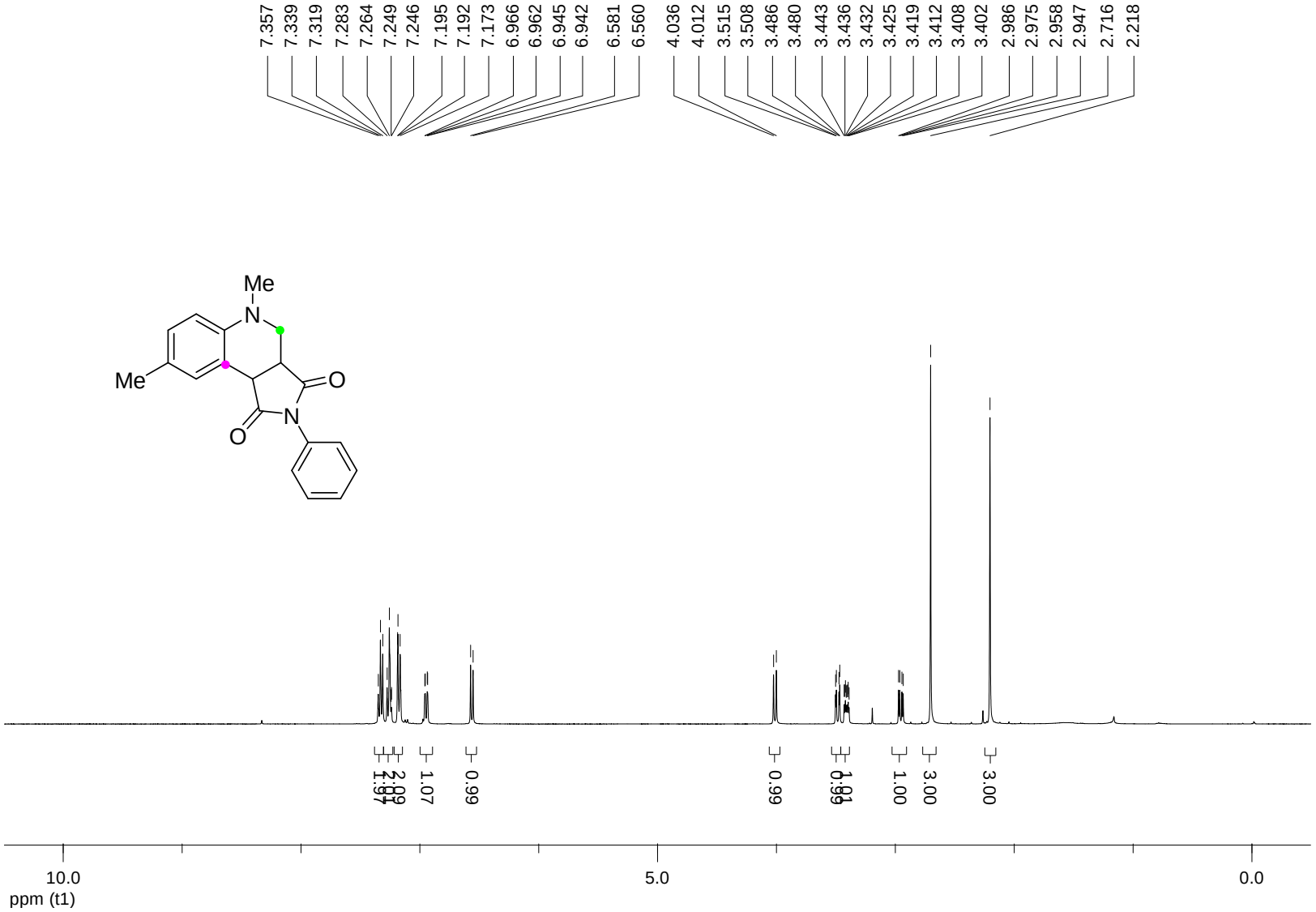

$^{13}$C NMR (100 MHz, $CDCl_3$) spectrum of **5g**

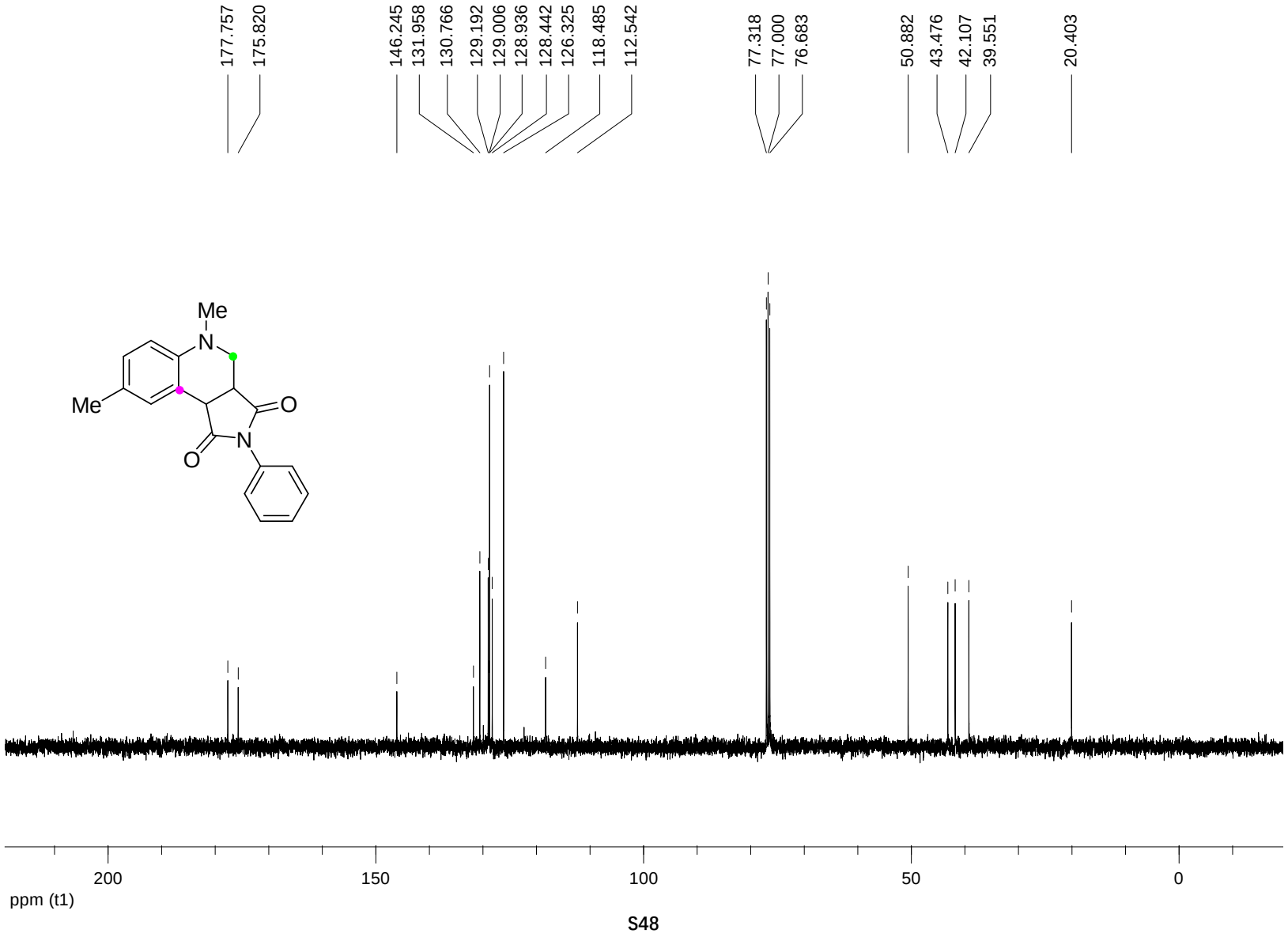

$^{1}$H NMR (400 MHz, $CDCl_3$) spectrum of **5h**

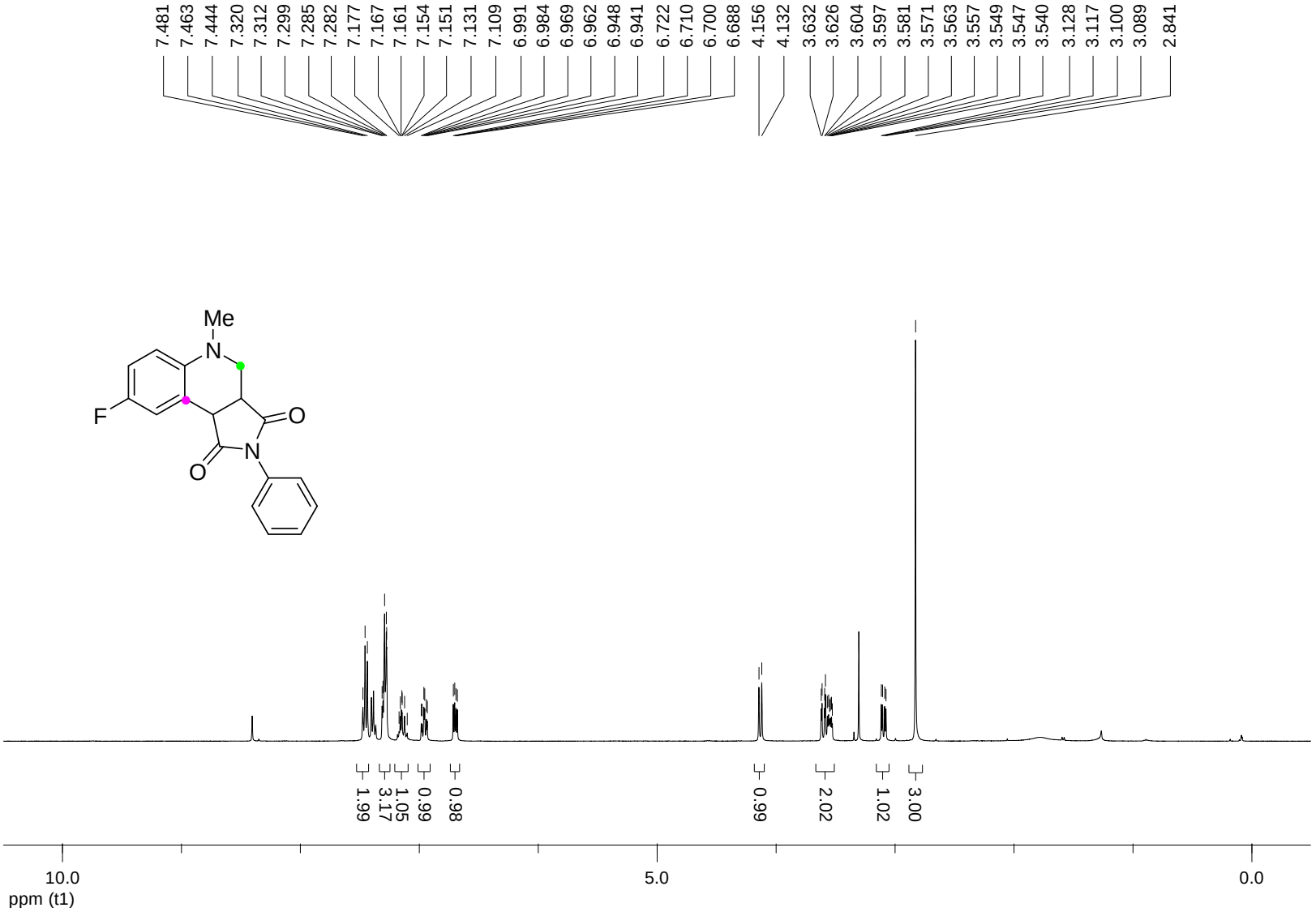

$^{13}C$ NMR (100 MHz, $CDCl_3$) spectrum of **5h**

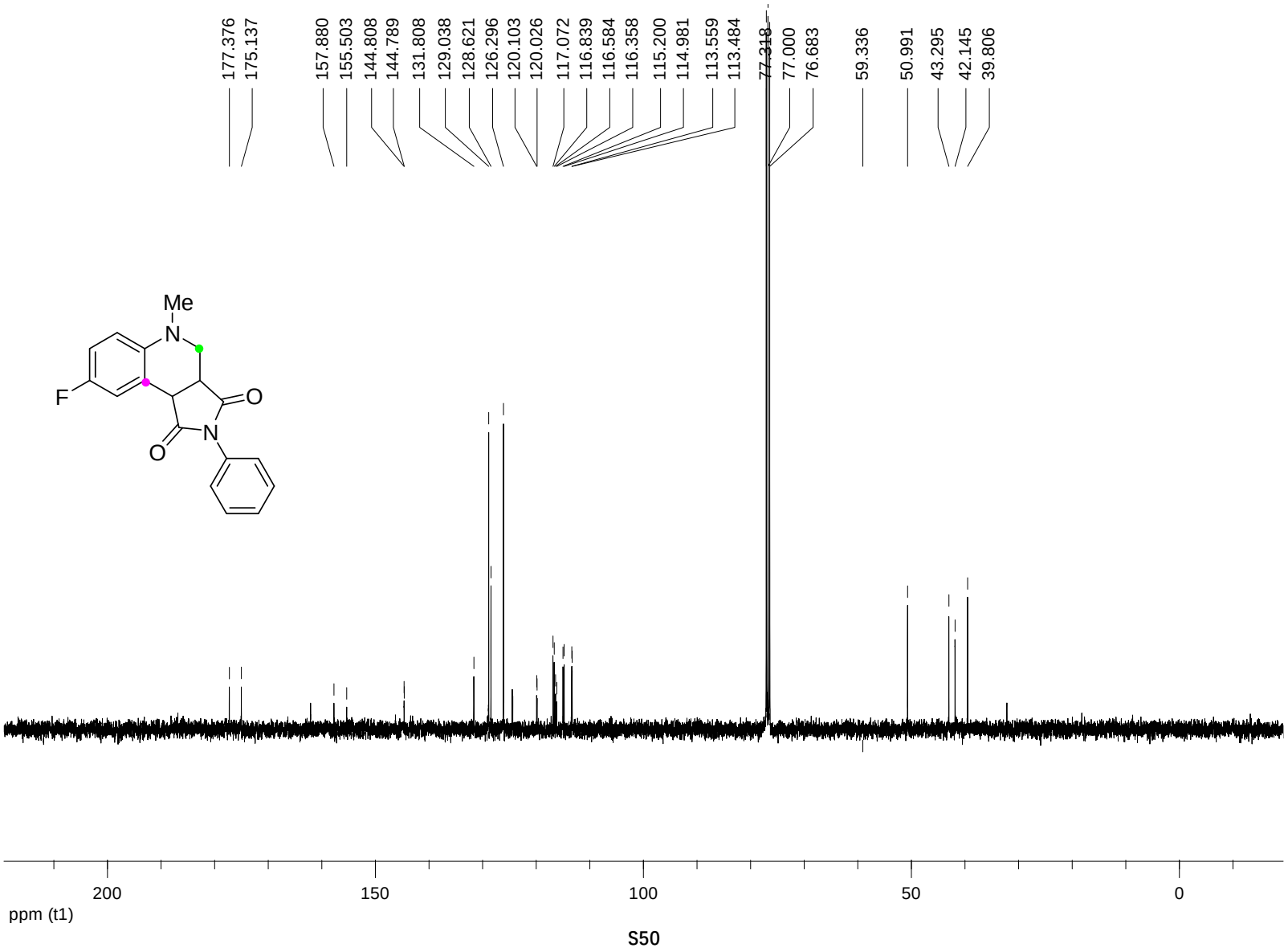

$^{1}$H NMR (400 MHz, $CDCl_3$) spectrum of **5i**

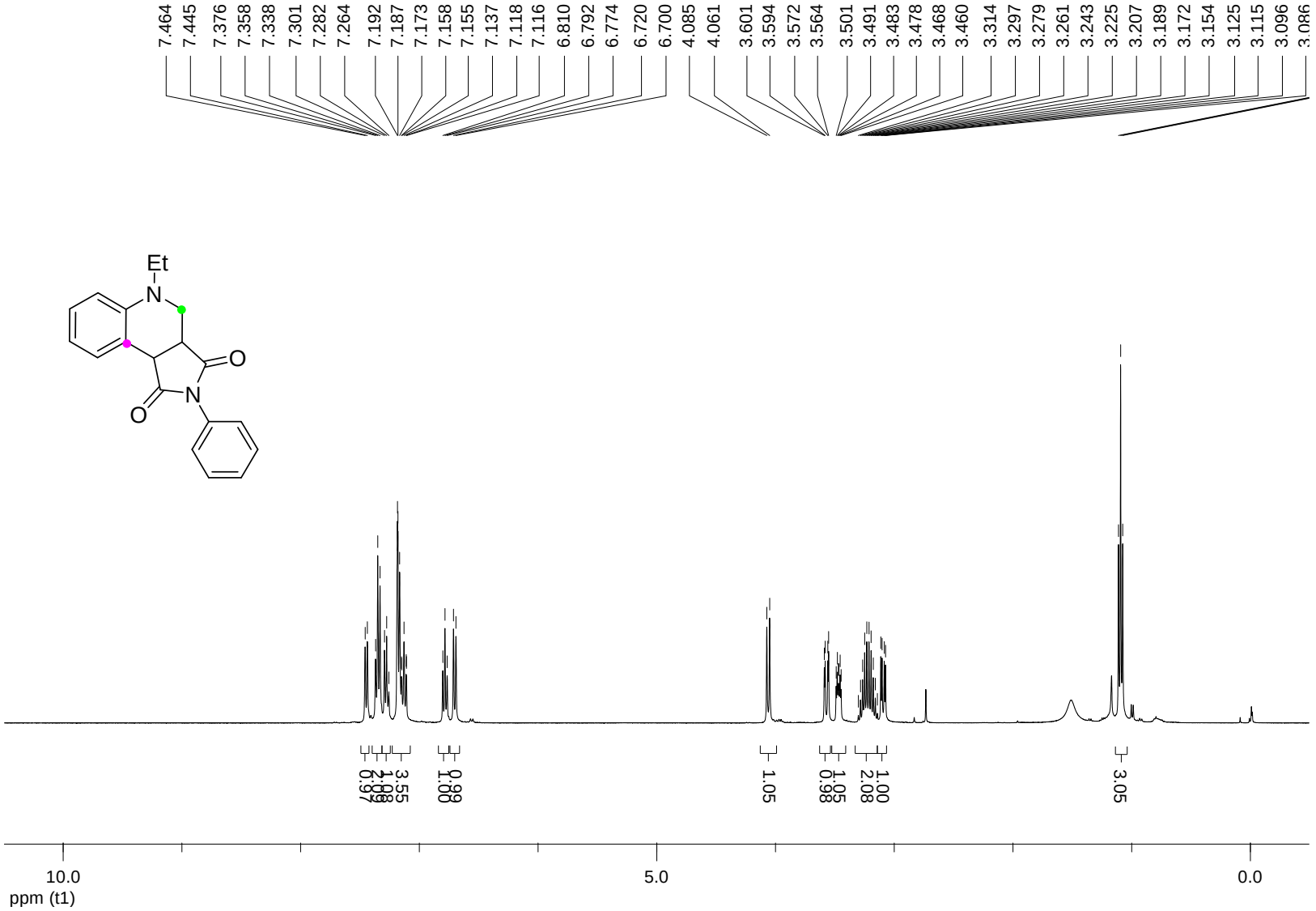

$^{13}C$ NMR (100 MHz, $CDCl_3$) spectrum of **5i**